

# Deuterium Exchange Reactions as a Probe of Biomolecule Structure. Fundamental Studies of Gas Phase H/D Exchange Reactions of Protonated Glycine Oligomers with D<sub>2</sub>O, CD<sub>3</sub>OD, CD<sub>3</sub>CO<sub>2</sub>D, and ND<sub>3</sub>

Sherrie Campbell, M. T. Rodgers, Elaine M. Marzluff, and J. L. Beauchamp\*

Contribution No. 8999 from the Arthur Amos Noyes Laboratory of Chemical Physics, California Institute of Technology, Pasadena, California 91125

Received October 25, 1994<sup>⊗</sup>

**Abstract:** A Fourier transform ion cyclotron resonance mass spectrometer was used to examine the hydrogen/deuterium exchange reactions of protonated glycine oligomers (Gly<sub>n</sub>, n = 1–5) with D<sub>2</sub>O, CD<sub>3</sub>OD, CD<sub>3</sub>CO<sub>2</sub>D, and ND<sub>3</sub>. Exchange rates in this study were monitored over three orders of magnitude, from 10<sup>-9</sup> to 10<sup>-12</sup> cm<sup>3</sup> molecule<sup>-1</sup> s<sup>-1</sup>. Reaction kinetics are highly dependent on peptide structure and the properties of the exchange reagents. The rate and extent of H/D exchange of the protonated oligomers increases with reagent gas basicity, D<sub>2</sub>O < CD<sub>3</sub>OD < CD<sub>3</sub>CO<sub>2</sub>D < ND<sub>3</sub>. ND<sub>3</sub> is the most efficient reagent studied, as it exchanges every labile hydrogen in each of the oligomers. Several distinct mechanisms, supported by semiempirical AM1 and PM3 calculations, are proposed to explain the observed patterns of reactivity. An onium ion mechanism is proposed for the exchange of N-terminus hydrogens of Gly<sub>n</sub>H<sup>+</sup> oligomers with ND<sub>3</sub>, in which an endothermic proton transfer from the N-terminus is rendered energetically feasible by simultaneous solvation of the resultant ammonium ion by the neutral peptide. This mechanism is consistent with the observation of multiple exchanges in a single collision event with ND<sub>3</sub>. For those reagents whose proton affinities are too low to form solvated onium ion intermediates, a relay mechanism is proposed in which the reagent shuttles a proton from the N-terminus to a slightly less basic site in the molecule. For glycine oligomers, this site is an amide oxygen. A tautomer mechanism is proposed for the exchange of the amide hydrogens with ND<sub>3</sub>. Exchange occurs by proton transfer from the N-terminus to the amide carbonyl in concert with transfer of the amide proton to ammonia, forming an ammonium ion solvated by a tautomerized peptide. Semiempirical calculations suggest that exchange of the C-terminus hydrogen proceeds via formation of a salt bridge with the reagent gas, which deprotonates the C-terminus acid group, with the nearby protonated N-terminus stabilizing the resultant ion pair. Betaine, [(CH<sub>3</sub>)<sub>3</sub>N<sup>+</sup>–CH<sub>2</sub>CO<sub>2</sub>H], used in this study to determine the isotopic purity of the exchange reagents, serves as a model for salt bridge formation since it does not possess a labile proton and readily exchanges the carboxylic acid hydrogen. The effect of translational and vibrational excitation on H/D exchange rates was studied for several oligomers using off-resonance collisional activation. For those oligomers that undergo facile H/D exchange with the reagent gases, excitation decreases rates. For those oligomers which do not undergo facile H/D exchange, reactivity is not promoted by collisional activation.

## Introduction

Conformational studies of peptides and proteins in solution have long been aided by isotopic labeling techniques.<sup>1</sup> For small peptides, solvent can access all the labile hydrogen sites and readily exchange the hydrogen for deuterium in the molecule. The rates of exchange can differ widely between the sites in the peptide, and have been shown to be a strong function of pH.<sup>2</sup> For large peptides in highly folded conformations, fewer labile hydrogen sites are exposed to the solvent for exchange, since many of the hydrogens are buried in the hydrophobic core of the protein.<sup>3</sup> Incorporation of deuterium at sites such as exposed amine, carboxylic acid, alcohol, and amide groups which react with differing rates has allowed structural determination via NMR spectroscopy.<sup>4</sup>

Although peptide and protein structures can be well characterized in solution, their gas-phase structures are virtually

unknown as there are relatively few experiments which extract this information. Employing the techniques of mass spectrometry, several research groups have used collision-induced dissociation to identify the amino acid composition and sequence of gas-phase peptides and proteins.<sup>5</sup> These experiments have been less useful in elucidating secondary structure information.

H/D exchange of biomolecules in solution has been employed to understand biophysical processes, with a recent emphasis on the kinetics and mechanisms of protein folding.<sup>6</sup> For example, in a fast-flow mixing system protein folding is initiated by dilution of a denaturant. After a suitable delay, the solution pH is raised to promote H/D exchange of exposed sites. In a final mixing step, the pH is lowered to terminate the exchange process. NMR, or more recently mass spectrometry,<sup>7</sup> is then used to examine the partially labeled protein molecules. With

\* Author to whom correspondence should be addressed (Email: jlbchamp@cco.caltech.edu).

<sup>⊗</sup> Abstract published in *Advance ACS Abstracts*, December 1, 1995.

(1) Werstiuk, N. H. *Isotopes in the Physical and Biomedical Sciences*; Elsevier: Amsterdam, 1987; Vol. 1, p 122.

(2) Wuthrich, K. *NMR of Proteins and Nucleic Acids*; Wiley-Interscience: New York, 1986.

(3) (a) Englander, S. W.; Kallenbach, N. R. *Q. Rev. Biophysics* 1984, 16, 521. (b) Roder, H. *Methods Enzymol.* 1989, 176, 446.

(4) See, for example: Roder, H.; Elove, G. A.; Englander, S. W. *Nature* 1988, 335, 700. Hughson, R. M.; Wright, P. E.; Baldwin, R. L. *Science* 1990, 249, 1544.

(5) (a) Biemann, K. *Methods in Enzymology*; McCloskey, J., Ed.; Academic Press: San Diego, CA, 1990; Vol. 193, p 351. (b) Johnson, R. S.; Martin, S. A.; Biemann, K. *Int. J. Mass Spectrom. Ion Processes* 1988, 86, 137. (c) Hunt, D. F.; Yates, J. R., III; Shabanowitz, J.; Winston, S.; Hauer, C. R. *Proc. Natl. Acad. Sci. U.S.A.* 1986, 83, 6233. (d) Schwartz, B. L.; Bursey, M. M. *Biol. Mass Spectrom.* 1991, 21, 92.

(6) Englander, S. W. *Science* 1993, 262, 848.

the advancements made in soft ionization techniques, such as electrospray<sup>8</sup> and fast atom bombardment,<sup>9</sup> examples of solution-phase H/D exchange of proteins followed by mass spectrometric analysis are abundant.<sup>10</sup> Although the proteins are detected in the gas phase, the extent of H/D exchange reflects the conformation in solution and does not necessarily have direct implications for gas-phase structures.

H/D exchange of simple molecules directly in the gas phase has been used extensively to distinguish between isomeric species,<sup>11,12</sup> to deduce reaction mechanisms,<sup>13,14,15</sup> and more recently to infer structural features of complex biomolecules.<sup>16,17</sup> Earlier studies from our laboratory,<sup>11</sup> using the technique of ion cyclotron resonance mass spectrometry, demonstrated for substituted benzene derivatives reacting with D<sub>2</sub>O that the rate of exchange was strongly dependent on the structure of the sample. For example, *o*- and *p*-xylene isomers exchanged all their labile hydrogens with rate constants of 10<sup>-11</sup> cm<sup>3</sup> molecule<sup>-1</sup> s<sup>-1</sup>, while *m*-xylene exchanged only one site more slowly. More recently, Ranasinghe *et al.*<sup>12</sup> investigated the H/D exchange of numerous protonated isomeric aromatic compounds in the collision region of a triple quadrupole mass spectrometer and determined that the proximity of the functional groups and the proton affinity difference between the analyte and the reagent gas were important factors in exchanging polyfunctional compounds. They concluded that ND<sub>3</sub> undergoes exchanges with all active hydrogens in the substituted aromatic compounds studied, even those remote from the charge site. For example, *p*-aminobenzoic acid exchanges all four labile hydrogens with ND<sub>3</sub> under trapped reaction conditions. In contrast, CH<sub>3</sub>OD displays proximity effects by only exchanging functional groups at specific orientations, and can be used to distinguish different isomers and functionalities. The same *p*-aminobenzoic acid undergoes only two exchanges with CD<sub>3</sub>OD, while *o*-aminobenzoic acid exchanges all form labile sites. More interestingly, they observed that exchange efficiencies for both reagent gases were highest whenever cluster species of the analyte and reagent were higher in abundance than the protonated analyte itself, indicating the importance of a collision complex for exchange.

Long-lived complexes are frequently postulated to account for the emergence of particular products from ion-molecule

reactions,<sup>18,19</sup> and a multiple-well potential energy surface<sup>20</sup> to describe H/D reactions has achieved general acceptance. Squires *et al.*<sup>21</sup> used this model over a decade ago to explain multiple H/D exchanges and determine reaction rate constants of anionic bases and neutral acids in flowing afterglow experiments. The potential energy surfaces drawn for simple H/D exchange are highly dependent on the proton affinity difference between the analyte and the deuterating reagent gas. For simple H/D exchange via proton transfer, exchange is most probable when the proton affinities of the reagent and the analyte molecule are similar. Investigations by Ausloos and Lias<sup>14</sup> have shown that for protonated monofunctional compounds, H/D exchange reactions do not occur when the proton affinities differ by more than 20 kcal/mol.

Several exceptions to this 20 kcal/mol limit have been shown for polyfunctional molecules, such as amino acids and peptides. Using the techniques of ion cyclotron resonance mass spectrometry, Gard *et al.*<sup>22</sup> demonstrated that H/D exchange of several protonated amino acids with CH<sub>3</sub>OD occurs despite proton affinity differences for the molecules of 30–40 kcal/mol. Most interesting is their finding that the exchange of the carboxylic acid occurs 3 to 10 times faster than the exchange of the more basic amino group, with rate constants ranging from 0.6 × 10<sup>-10</sup> to 1.4 × 10<sup>-10</sup> cm<sup>3</sup> molecule<sup>-1</sup> s<sup>-1</sup>. Cheng and Fenselau<sup>23</sup> investigated the H/D exchange of four protonated peptides, ranging in proton affinity from 234 to ≥255 kcal/mol, with ND<sub>3</sub> in a four sector tandem mass spectrometer. Despite proton affinity differences of greater than 50 kcal/mol, all peptides underwent complete or partial exchange with the reagent gas. Their results from varying collision gas pressure and collision energy reconfirm the importance of a collision complex for H/D exchange.

Winger *et al.*<sup>16</sup> reported perhaps the first gas-phase H/D exchange results for protein ions. Multiply protonated bovine proinsulin and α-lactalbumin were generated using electrospray ionization and reacted with D<sub>2</sub>O in a "reaction capillary" prior to detection using a triple quadrupole mass spectrometer. The native and disulfide bond reduced forms of the protein displayed different reactivities in the gas phase with the D<sub>2</sub>O exchange reagent, allowing the different protein conformations to be distinguished according to their reactivity. Suckau *et al.*<sup>17</sup> probed the gas-phase reactivity of multiply protonated cytochrome *c* formed by electrospray ionization with D<sub>2</sub>O using an ion cyclotron resonance mass spectrometer. Their exchange results were interpreted to indicate that more than one molecular conformation can exist for a specific mass to charge species in a spectrum. Suckau *et al.*<sup>17</sup> suggested that gas-phase species with distinctive exchange reactivity could be correlated with known solution-phase structures.

The rates of H/D exchange for cytochrome *c* were also reported, and varied from 5 × 10<sup>-13</sup> to 2 × 10<sup>-12</sup> cm<sup>3</sup> molecule<sup>-1</sup> s<sup>-1</sup> depending on the charge state of the ion. Rates increased almost linearly with the number of charges on the

(7) Miranker, A.; Robinson, C. V.; Radford, S. E.; Aplin, R. T.; Dobson, C. M. *Science* **1993**, *262*, 896.

(8) (a) Fenn, J. B.; Mann, M.; Meng, C. K.; Wong, S. F.; Whitehouse, C. M. *Science* **1989**, *246*, 64. (b) Smith, R. D.; Loo, J. A.; Loo, R. R. O.; Busman, M.; Udseth, H. R. *Mass Spectrom. Rev.* **1991**, *10*, 359.

(9) (a) Barber, M.; Bordoli, R. S.; Sedgwick, R. D.; Vickerman, J. J. *J. Chem. Soc., Faraday Trans.* **1982**, *78*, 1291. (b) Barber, M.; Bordoli, R. S.; Sedgwick, R. D.; Tyler, A. N. *J. Chem. Soc., Chem. Commun.* **1981**, 325.

(10) (a) Katta, V.; Chait, B. T. *Proceeding of the 39th Conference Mass Spectrometry and Allied Topics*; Nashville, TN; ASMS: East Lansing, MI, 1991; p 1247. (b) Katta, V.; Chait, B. T. *Rapid Commun. Mass Spectrom.* **1991**, *5*, 214. (c) Katta, V.; Chait, B. T. *J. Am. Chem. Soc.* **1993**, *115*, 6317. (d) Verma, S.; Pomerantz, S. C.; Sethi, S. K.; McCloskey, J. A. *Anal. Chem.* **1986**, *58*, 2898. (e) Sepetov, N. F.; Issakova, O. L.; Lebl, M.; Swiderek, K.; Stahl, D. C.; Lee, T. D. *Rapid Commun. Mass Spectrom.* **1993**, *7*, 58. (f) Guarini, A.; Guglielmetti, G.; Andriollo, N.; Vincenti, M. *Anal. Chem.* **1992**, *64*, 204.

(11) Freiser, B. S.; Woodin, R. L.; Beauchamp, J. L. *J. Am. Chem. Soc.* **1975**, *97*, 6893.

(12) Ranasinghe, A.; Cooks, R. G.; Sethi, S. K. *Org. Mass Spectrom.* **1992**, *27*, 77.

(13) Squires, R. R.; Bierbaum, V. M.; Grabowski, J. J.; DePuy, C. H. *J. Am. Chem. Soc.* **1983**, *105*, 5185.

(14) (a) Ausloos, P.; Lias, S. G. *J. Am. Chem. Soc.* **1981**, *103*, 3641. (b) Lias, S. G. *J. Phys. Chem.* **1984**, *88*, 4401.

(15) Hunt, D. F.; Sethi, S. K. *J. Am. Chem. Soc.* **1980**, *102*, 6953.

(16) Winger, B. E.; Light-Wahl, K. J.; Rockwood, A. L.; Smith, R. D. *J. Am. Chem. Soc.* **1992**, *114*, 5897.

(17) Suckau, D.; Shi, Y.; Beu, S. C.; Senko, M. W.; Quinn, J. P.; Wampler, F. M.; McLafferty, F. W. *Proc. Natl. Acad. Sci.* **1993**, *90*, 790.

(18) Meot-Ner, M. *Molecular Structures and Energetics*; VCH Publishers: New York, 1986; Vol. 4, p 71.

(19) (a) Bohme, D. K. *Interactions Between Ions and Molecules*; Plenum: New York, 1975; p 489. (b) Farneth, W. E.; Brauman, J. I. *J. Am. Chem. Soc.* **1976**, *98*, 7891.

(20) (a) Olmstead, W. N.; Brauman, J. I. *J. Am. Chem. Soc.* **1977**, *99*, 4219. (b) Asubiojo, O. I.; Brauman, J. I. *J. Am. Chem. Soc.* **1979**, *101*, 3715.

(21) Squires, R. R.; Bierbaum, V. M.; Grabowski, J. J.; DePuy, C. H. *J. Am. Chem. Soc.* **1983**, *105*, 5185.

(22) (a) Gard, E.; Willard, D.; Green, M. K.; Bregar, J.; Lebrilla, C. B. *Org. Mass Spectrom.* **1993**, *28*, 1632. (b) Gard, E.; Green, M. K.; Bregar, J.; Lebrilla, C. B. *J. Am. Soc. Mass Spectrom.* **1994**, *5*, 614.

(23) Cheng, X.; Fenselau, C. *Int. J. Mass Spectrom. Ion Processes* **1992**, *122*, 109.

molecules. In comparison with the rates of most ion–molecule reactions, these exchange processes are rather slow. We will consider exchange reactions which proceed with rate constants in excess of  $10^{-10}$  cm<sup>3</sup> molecule<sup>-1</sup> s<sup>-1</sup> as facile since they take place with fewer than 10 collisions. In contrast, when  $10^3$  or more collisions are required for exchange (corresponding to rates  $\leq 10^{-12}$  cm<sup>3</sup> molecule<sup>-1</sup> s<sup>-1</sup>), reactions are not facile in that features must be present in the potential energy surface which inhibit access to the transition state for the process during the lifetime of the collision complex.

Distinctive chemical reactivity remains the principle experimental method to probe the structures of complex molecule ions in the gas phase. Other than adduct formation and simple processes such as proton transfer, there is little known about the gas-phase ion chemistry of biological molecules. Isotopic hydrogen exchange reactions are the only notable exception. With the limited range of studies that have been performed to date, very little is known about the mechanism and energetics of H/D exchange processes for complex molecules.

We have undertaken a systematic study of isotopic hydrogen exchange using FT-ICR techniques, focusing our attention on simple glycine oligomers (Gly<sub>n</sub>,  $n = 1-5$ ) reacting with a series of reagent gases. The glycine oligomers are ideal model systems for understanding the mechanisms of H/D exchange. The glycine residues do not have basic side chains, hence the site of protonation in all the oligomers studied is the N-terminus nitrogen. Additionally, there have been several recent measurements of the gas-phase proton affinities for this series.<sup>24-26</sup> The proton affinities reported for Gly<sub>1</sub> to Gly<sub>5</sub> via the kinetic method are 211.6, 219.1, 223.1, 227.2, and 231.8 kcal/mol, respectively.<sup>24</sup> The choice of H/D exchange gases reflects our attempt to probe a range of proton affinities and include species which are capable of multiple exchanges in a single encounter.<sup>27</sup> The reagents investigated include D<sub>2</sub>O (166.5), CD<sub>3</sub>OD (181.9), CD<sub>3</sub>-CO<sub>2</sub>D (190.2), and ND<sub>3</sub> (204.0 kcal/mol).<sup>28</sup> In this article, a kinetic analysis of the deuterium incorporation data for all five oligomers with each reagent gas is presented.<sup>29</sup> The simplicity of the glycine oligomers facilitates theoretical studies to better understand our experiments. We have modeled our results using semiempirical AM1<sup>30</sup> and PM3<sup>31</sup> calculations to quantify reaction coordinate diagrams for selected systems. We wish to report findings which assist in elucidating important features of potential energy surfaces for isotopic hydrogen exchange and stable structures of peptides in the gas phase.

(24) Wu, Z.; Fenselau, C. *J. Am. Soc. Mass Spectrom.* **1992**, *3*, 863.

(25) Wu, J.; Lebrilla, C. *J. Am. Chem. Soc.* **1993**, *115*, 3270.

(26) Zhang, K.; Zimmerman, D. M.; Chung-Phillips, A.; Cassidy, C. *J. Am. Chem. Soc.* **1993**, *115*, 10812.

(27) For examples of multiple exchanges in a single collision event, see: Grabowski, J. J.; DePuy, C. H.; Van Doren, J. M.; Bierbaum, V. M. *J. Am. Chem. Soc.* **1985**, *107*, 7384.

(28) A compilation of gas phase basicities and proton affinities can be found in: Lias, S. G.; Bartmess, J. E.; Liebman, J. F.; Holmes, J. L.; Levin, R. D.; Mallard, W. G. *J. Phys. Chem. Ref. Data* **1988**, *17*(1).

(29) Preliminary results have been previously presented, see: Campbell, S.; Rodgers, M. T.; Marzluff, E. M.; Beauchamp, J. L. *J. Am. Chem. Soc.* **1994**, *116*, 9765.

(30) (a) Dewar, M. J. S.; Zoebisch, E. G.; Healy, E. F.; Stewart, J.-J. P. *J. Am. Chem. Soc.* **1985**, *107*, 3902. (b) Dewar, M. J. S.; Dieter, K. M. *J. Am. Chem. Soc.* **1986**, *108*, 8075.

(31) (a) Stewart, J. J. P. *Method J. Comput. Chem.* **1989**, *10*, 209. (b) Stewart, J. J. P. *Method J. Comput. Chem.* **1989**, *10*, 221.

(32) (a) Campbell, S.; Marzluff, E. M.; Rodgers, M. T.; Beauchamp, J. L.; Rempe, M. E.; Schwinck, K. F.; Lichtenberger, D. L. *J. Am. Chem. Soc.* **1994**, *116*, 5257. (b) Marzluff, E. M.; Campbell, S.; Rodgers, M. T.; Beauchamp, J. L. *J. Am. Chem. Soc.* **1994**, *116*, 7787. (c) Rodgers, M. T.; Campbell, S.; Marzluff, E. M.; Beauchamp, J. L. *Int. J. Mass Spectrom. Ion Processes* **1994**, *137*, 121.

## Experimental Details

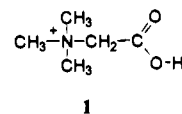
Experiments were performed in an external ion source Fourier transform ion cyclotron resonance (FT-ICR) mass spectrometer. A detailed description of this instrument has been previously published.<sup>32</sup> The spectrometer incorporates a Cs ion bombardment source, octopole ion guide for transferring ions into the high-field region of a 7-T superconducting magnet, a standard  $2 \times 2 \times 3$  in.<sup>3</sup> detection cell, and the electronics required for data acquisition and processing in the Fourier transform mode. The instrument has three regions of differential cryogenic pumping, resulting in a residual background pressure of high  $10^{-10}$  or low  $10^{-9}$  Torr in the detection cell. A Schulz-Phelps ionization gauge is an integral part of the ICR cell and is calibrated using a capacitance manometer connected directly to the cell through a static port. Uncertainties in pressure measurements are estimated to be  $\pm 20\%$ . This is the major source of error in reported rate constants. Comparison of literature rates for several well-characterized reactions to measurements made with the new instrument give agreement within this range of uncertainty. Deuterating gases are degassed using several freeze–thaw cycles before introduction directly into the ICR cell using Varian leak valves. Typical static gas pressures used in the exchange reactions are  $(0.5-1.5) \times 10^{-7}$  Torr. Higher pressures lead to significant ion losses at long trapping times.

Samples are typically prepared by dissolving small amounts of solid ( $\sim 0.1$  mg) directly into a 2–3- $\mu$ L drop of a mixture of glycerol and trifluoroacetic acid spread onto a copper probe tip. Protonated peptide ions are produced by Cs ion bombardment of the acidic matrix and are transported and loaded into the ICR cell for 100 ms. Species are isolated within 20 ms of the ion loading period by applying rf excitation at the resonance frequencies of all unwanted higher and lower mass ions in the ICR cell. Fast ion bombardment can generate ions with a full range of excess vibrational energy. Evidence for this has been provided by various experiments which reported the metastable decay of large ions over several milliseconds.<sup>33</sup> In our experiments, the peptide ions were not observed to decompose after isolation. The effects of excess vibrational and translational energies of reactant ions are further considered below.

To avoid off-resonance excitation<sup>34</sup> of the reactant ion, carbon-13 isotopes of the protonated glycine oligomers were not ejected from the cell. All isotopic contributions were subtracted from the raw data (according to their natural abundances) prior to calculating the reaction rate constants. H/D exchange reaction times were varied from a minimum of 130 ms up to 20 s.

Methyl esters of the glycine oligomers were synthesized by dissolving the peptides in a solution of methanol and trifluoroacetic acid (99:1) and stirring overnight. Reaction yields did not exceed 75%, but products could be easily isolated in the FT-ICR experiments. Structures of the products were confirmed using collision-induced dissociation techniques. All other peptide samples were commercially available from Sigma Chemical Co. and used as provided without further purification. The deuterating reagents D<sub>2</sub>O (99.9 atom % deuterium), CD<sub>3</sub>OD (99.8 atom % deuterium), and CD<sub>3</sub>CO<sub>2</sub>D (99.91 atom % deuterium) were also purchased from Sigma Chemical Co. ND<sub>3</sub> was obtained from Matheson with a purity of 99.0 atom % deuterium.

Since our FT-ICR instrument is not exclusively used for H/D exchange reactions, the vacuum chamber is primed overnight with deuterating gas at approximately  $10^{-6}$  Torr to allow for the complete exchange of all surfaces. Although the reagent gases have high isotopic purity ( $>99$  atom %) prior to introduction into mass spectrometer, the percent deuterium of the reagent gases in the vacuum chamber is not as high. A unique molecule for probing the percent deuterium of each reagent gas in the vacuum chamber is betaine (Structure 1). Since



(33) (a) Ngoka, L. C.; Gal, J. F.; Lebrilla, C. B. *Anal. Chem.* **1994**, *66*, 692. (b) Ngoka, L. C.; Lebrilla, C. B. *J. Am. Soc. Mass Spectrom.* **1993**, *4*, 210.

(34) Gauthier, J. W.; Trautman, T. R.; Jacobson, D. B. *Anal. Chim. Acta* **1991**, *246*, 211.

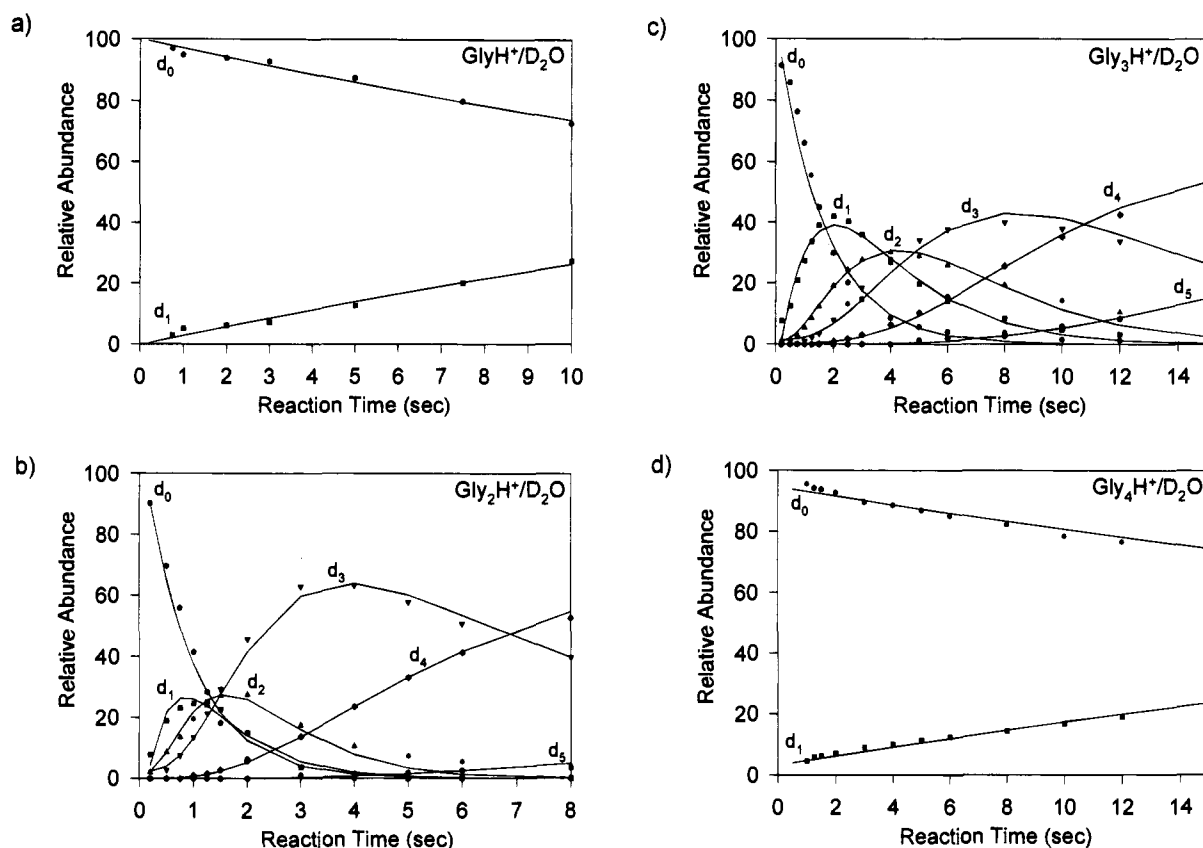


**Figure 1.** Time plots of the H/D exchange products of  $\text{Gly}_n\text{H}^+$  with  $\text{D}_2\text{O}$  ( $1.0 \times 10^{-7}$  Torr). (a)  $\text{GlyH}^+$  exchanges only one hydrogen slowly with  $\text{D}_2\text{O}$ . (b) In contrast,  $\text{Gly}_2\text{H}^+$  readily exchanges all five labile hydrogens. (c)  $\text{Gly}_3\text{H}^+$  exchanges five or six labile hydrogens. (d) Facile exchange abruptly halts, as  $\text{Gly}_4\text{H}^+$  slowly exchanges a single hydrogen. Least-squares fits (lines) of the kinetic equation (see text) to the experimental intensities (points) are shown. The number of deuterium atoms incorporated into each species is indicated as  $d_n$ .

betaine contains one labile hydrogen which exchanges fairly rapidly, the product ion distribution after complete H/D exchange indicates the actual atom percent deuterium of the reagent gas in the vacuum chamber. For all reagent gases studied, the percent deuterium ranged from 90 to 95 atom %.

Semiempirical calculations were performed with Hyperchem<sup>35</sup> to obtain model structures and energetics for the protonated glycine oligomers and the reagent exchange gases. Both the AM1<sup>30</sup> and PM3<sup>31</sup> semiempirical methods were employed. In all of the calculations, starting structures for the molecules were obtained using the standard amino acid templates provided with Hyperchem. Structures for the protonated species were obtained by attaching a proton to a basic site. The structure was then annealed using molecular mechanics and energy minimized using semiempirical methods. The site of protonation and initial geometry was varied to determine the differences in the structure and stability of various conformations of the protonated parent molecules. Geometries of the protonated peptide/reagent gas adducts, neutral peptides, and reagent gases were obtained in a similar manner. Since both the AM1 and PM3 methods give a very poor estimate of the heat of formation of  $\text{H}^+$ , the experimental value of 365.7 kcal/mol was used.<sup>28</sup>

## Results

**Reactions with  $\text{D}_2\text{O}$ .**  $\text{D}_2\text{O}$ , with a proton affinity of 166.5 kcal/mol,<sup>28</sup> is the least basic exchange reagent used in this study. The differences in proton affinity between  $\text{D}_2\text{O}$  and the glycine oligomers ( $n = 1-5$ ) range from 45.1 to 65.3 kcal/mol.<sup>24</sup>  $\text{Gly}_1\text{H}^+$ , with the smallest difference in proton affinities, is virtually unreactive with  $\text{D}_2\text{O}$ , displaying one slow exchange of a labile hydrogen during the 10-s reaction period (Figure 1a).  $\text{Gly}_2\text{H}^+$  is more reactive with  $\text{D}_2\text{O}$ , since all five of its

labile hydrogens are observed to exchange (Figure 1b). Three of five H/D exchangers are fairly fast, proceeding within the first 3 s of reaction, while the remaining exchanges are slower. The reaction of  $\text{Gly}_3\text{H}^+$  with  $\text{D}_2\text{O}$  is slightly less efficient than that of  $\text{Gly}_2\text{H}^+$ , since only five of six labile hydrogens are observed to exchange (Figure 1c). ( $\text{Gly}_3\text{-OMe}$ ) $\text{H}^+$  exchanges all five of its labile hydrogens with  $\text{D}_2\text{O}$ , possibly indicating the unreactive sixth site on  $\text{Gly}_3\text{H}^+$  is the C-terminus hydroxyl. For the larger oligomers  $\text{Gly}_4\text{H}^+$ , ( $\text{Gly}_4\text{-OMe}$ ) $\text{H}^+$ , and  $\text{Gly}_5\text{H}^+$  reacting with  $\text{D}_2\text{O}$ , facile exchange abruptly halts and only one deuterium is slowly incorporated into the molecule (e.g., Figure 1d). Since the proton affinity of  $\text{Gly}_4\text{H}^+$  is reported as 227.2 kcal/mol, an upper limit of 61 kcal/mol can be implied as the largest difference in proton affinities for which H/D exchange occurs with  $\text{D}_2\text{O}$ . Two observations can be made from the exchange data with  $\text{D}_2\text{O}$ . First, excluding glycine, H/D exchange rates decrease with increasing proton affinity of the peptide. Second, a subtle change to the oligomer (addition of a single glycine unit to  $\text{Gly}_3$ ) can cause a dramatic change in reactivity.

It is of interest to explore the occurrence of multiple exchanges in a single collision event.  $\text{D}_2\text{O}$  has the opportunity to exchange two deuteriums during each reactive encounter. Of the glycine oligomers studied, only  $\text{Gly}_2$  and  $\text{Gly}_3$  exchange more than a single site with  $\text{D}_2\text{O}$ . Figure 2a shows the results of reacting  $\text{Gly}_3\text{H}^+$  with  $\text{D}_2\text{O}$  for 1 s. Three deuteriums are incorporated into the oligomer during this time period. If the  $d_1$  species ( $m/z = 191$ , resulting from one exchange) is continuously ejected during the 1 s time period, no higher mass products are observed (Figure 2b). Under similar experimental conditions,  $\text{Gly}_2\text{H}^+$  also displays no higher mass products when

(35) Hyperchem Computational Software Package, Ver. 4.0; Hypercube Inc., 1994. For a review of this computational package, see: Froimowitz, M. *Biotechniques* 1993, 14, 1010.

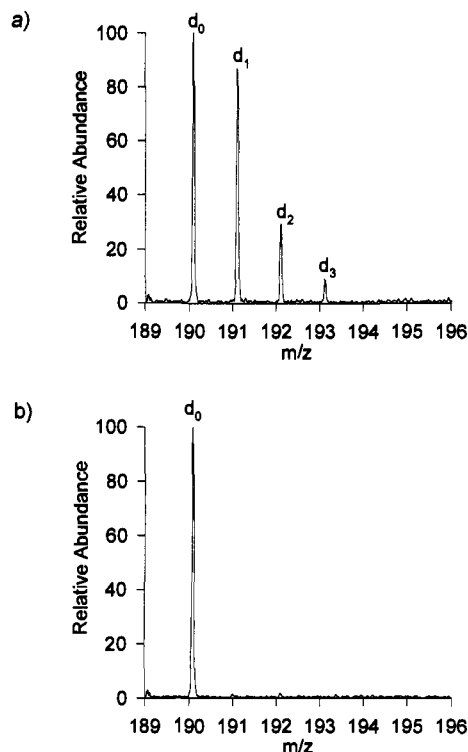


**Figure 2.** (a) H/D exchange products of  $\text{Gly}_3\text{H}^+$  with  $\text{D}_2\text{O}$  ( $1.0 \times 10^{-7}$  Torr) after 1 s. (b) Continuous ejection of the  $d_1$  ( $m/z = 191$ ) species during the reaction inhibits formation of higher mass exchange products.  $\text{D}_2\text{O}$  partakes in primarily single, sequential exchanges.

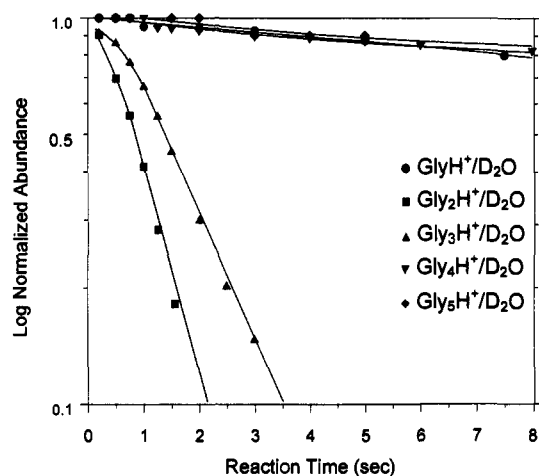


**Figure 3.** Semilog plots of ion abundance versus reaction time for  $\text{Gly}_n\text{H}^+$  with  $\text{D}_2\text{O}$  ( $1.0 \times 10^{-7}$  Torr). Reaction rate constants for the first exchange are extracted from the limiting slope of each plot. H/D exchange of  $\text{Gly}_2$  and  $\text{Gly}_3$  is an order of magnitude faster than that of  $\text{Gly}_1$ ,  $\text{Gly}_4$ , and  $\text{Gly}_5$ . Curvature in the slopes at short delays indicates a vibrationally and translationally hot population with decreased reactivity, which cools after approximately 500 ms.

continuously ejecting the  $d_1$  species.  $\text{D}_2\text{O}$  therefore partakes in predominantly single, sequential exchanges with the glycine oligomers.

Determination of the reaction rate constants for glycine oligomers with  $\text{D}_2\text{O}$  is straightforward, and similar to the approach used by Gard et al.<sup>22</sup> The above experiment provides support for calculating these values using a model of simple sequential deuterium incorporation. The rate constant for the exchange of the nascent reactant  $\text{MH}^+$  can be determined from the slope of a semilog plot of ion abundance versus reaction time. Data for  $\text{Gly}_n\text{H}^+$  ( $n = 1-5$ ) are shown in Figure 3. The reaction rate constants for the first exchanges are  $1.8 \times 10^{-11}$ ,  $3.7 \times$

$10^{-10}$ ,  $2.5 \times 10^{-10}$ ,  $1.5 \times 10^{-11}$ , and  $2.0 \times 10^{-11}$   $\text{cm}^3 \text{ molecule}^{-1} \text{ s}^{-1}$  for  $\text{Gly}_1\text{H}^+$  to  $\text{Gly}_5\text{H}^+$ , respectively, taken from limiting slopes for the disappearance of the reactant ion in Figure 3. These results are summarized in Table 1. The curvature of the plots at short times suggests a translationally or vibrationally hot population which reacts more slowly than thermalized ions.<sup>36</sup> The long time behavior for each plot should approach that of a thermal distribution. There are not indications of an unreactive population in any of the systems, which might suggest that only species with excess energy react.

To determine the reaction rate constants for subsequent sequential exchanges, the data can be fit using mathematical modeling. For  $n$  exchangeable hydrogens, a series of  $n + 1$  coupled first-order differential equations is solved numerically to yield  $n + 1$  curves describing the time-dependent behavior of the different deuterated species. Rate constants which give a best fit to the experimental data are summarized in Table 1. The equations can be modified to account for reverse reactions which regenerate lower mass hydrogenated peptides if the concentration of HOD is found to be significant in the background gas. Results from calculations which include this correction do not vary significantly from the simpler model, since the isotopic impurities do not typically exceed 5–10 atom %.

As an alternate method, the  $k_2$  and  $k_3$  rate constants of  $\text{Gly}_2\text{H}^+$  and  $\text{Gly}_3\text{H}^+$  can be estimated from the exchange time plots in Figure 1, parts b and c. The peak in the curve for the  $d_1$  species occurs at a reaction time where product formation and depletion rates are equal, which happens when eq 1 is satisfied. This yields  $k_2$  values for  $\text{Gly}_2\text{H}^+$  and  $\text{Gly}_3\text{H}^+$  of  $5.8 \times 10^{-10}$  and  $1.5 \times 10^{-10}$   $\text{cm}^3 \text{ molecule}^{-1} \text{ s}^{-1}$ , respectively, as compared with the values of  $5.2 \times 10^{-10}$  and  $1.4 \times 10^{-10}$   $\text{cm}^3 \text{ molecule}^{-1} \text{ s}^{-1}$  in Table 1. The  $k_3$  rate constants can be estimated in a similar manner from the ion abundances at the maximum in the yield of  $d_2$ , eq 2. This gives  $k_3$  values for  $\text{Gly}_2\text{H}^+$  and  $\text{Gly}_3\text{H}^+$  of  $3.9 \times 10^{-10}$  and  $1.3 \times 10^{-10}$   $\text{cm}^3 \text{ molecule}^{-1} \text{ s}^{-1}$ , respectively, compared with best fit values of  $3.6 \times 10^{-10}$  and  $1.2 \times 10^{-10}$   $\text{cm}^3 \text{ molecule}^{-1} \text{ s}^{-1}$  from Table 1. It is interesting to note that the data for  $\text{Gly}_2\text{H}^+$  in Figure 1b indicate that  $k_2$  is faster than  $k_1$ .

$$k_2 = k_1 \frac{[d_0]}{[d_1]} \quad (1)$$

$$k_3 = k_2 \frac{[d_1]}{[d_2]} \quad (2)$$

The calculated ADO reaction rates<sup>37</sup> for each species are included for comparison to the experimental values in Table 1. The species which undergo only a single exchange with  $\text{D}_2\text{O}$  [ $\text{GlyH}^+$ ,  $\text{Gly}_4\text{H}^+$ ,  $(\text{Gly}_4\text{-OMe})\text{H}^+$ , and  $\text{Gly}_5\text{H}^+$ ] all possess similar rate constants in the range of  $10^{-11}$  to  $10^{-12}$   $\text{cm}^3 \text{ molecule}^{-1} \text{ s}^{-1}$ , much slower than the ADO collision limit.  $\text{Gly}_2\text{H}^+$ ,  $\text{Gly}_3\text{H}^+$ , and  $(\text{Gly}_3\text{-OMe})\text{H}^+$  display similar reactivity with three moderately fast exchanges of  $10^{-10}$   $\text{cm}^3 \text{ molecule}^{-1} \text{ s}^{-1}$ , and two slower reactions.

Conceptually it is easy to think that the initial H/D exchange occurs at the most reactive site. In fact, even though some sites have a higher probability of exchange in the first event, the "first" exchange does not necessarily have to occur at any one

(36) Examples of this behavior have been previously reported in: Blint, R. J.; McMahon, T. B.; Beauchamp, J. L. *J. Am. Chem. Soc.* **1974**, *96*, 1269.

(37) Bowers, M. T. *Gas Phase Ion Chemistry*; Academic Press: New York, 1979; Vol. 1, Chapter 3.

**Table 1.** H/D Exchange Rates for Glycine Oligomers with Reagent Gases Using a Sequential Model for Deuterium Incorporation (rates  $\times 10^{10}$  cm<sup>3</sup>/s)

gas	Gly <sub>n</sub>	ADO rate	no. of observed deuterium exchanges								
			d <sub>1</sub> <sup>a</sup>	d <sub>2</sub>	d <sub>3</sub>	d <sub>4</sub>	d <sub>5</sub>	d <sub>6</sub>	d <sub>7</sub>	d <sub>8</sub>	
D <sub>2</sub> O	betaine	17.2	0.01	—	—	—	—	—	—	—	—
	1	17.9	0.09 (0.18)	*	*	*	*	*	*	*	*
	2	17.0	3.1 (3.7)	5.2	3.6	0.47	0.07	—	—	—	—
	3	16.7	1.8 (2.5)	1.4	1.2	0.47	0.12	*	—	—	—
	3-Me	16.7	1.6	1.2	1.1	0.36	0.07	—	—	—	—
MeOD	4	16.5	0.05 (0.15)	*	*	*	*	*	*	*	*
	4-Me	16.5	0.04	*	*	*	*	*	*	*	*
	5	16.4	0.02 (0.20)	*	*	*	*	*	*	*	*
	betaine	14.7	1.0	—	—	—	—	—	—	—	—
	1	15.6	1.9 (2.7)	0.78	0.55	0.25	—	—	—	—	—
AcOD	2	14.5	5.0 (6.1)	8.8	5.6	1.7	0.78	—	—	—	—
	3	14.0	4.3 (4.6)	4.6	3.4	1.2	0.32	0.16	—	—	—
	3-Me	14.0	2.1	2.3	1.6	0.49	0.13	—	—	—	—
	4	13.8	0.23 (0.48)	0.21	*	*	*	*	*	*	*
	4-Me	13.8	0.02	0.04	*	*	*	*	*	*	*
ND <sub>3</sub>	5	13.6	0.01 (0.03)	*	*	*	*	*	*	*	*
	betaine	12.9	2.5	—	—	—	—	—	—	—	—
	1	14.1	4.5	1.5	1.1	0.53	—	—	—	—	—
	2	12.7	10.2 (11.8)	8.8	5.6	1.9	0.72	—	—	—	—
	3	12.0	7.4	5.2	4.0	2.0	0.78	0.34	—	—	—
CD <sub>3</sub> OD	4	11.7	1.4 (4.5)	0.43	0.40	0.39	*	*	*	*	*
	5	11.4	3.5 (5.3)	0.35	0.36	0.40	*	*	*	*	*
	betaine	13.8	2.1	—	—	—	—	—	—	—	—
	1	14.3	2.7 (3.4)	5.5	3.6	1.1	—	—	—	—	—
	2	13.7	5.4 (7.4)	8.1	5.0	2.1	0.39	—	—	—	—
CD <sub>3</sub> CO <sub>2</sub> D	3	13.4	8.9 (10.3)	14.1	11.9	7.2	2.8	0.47	—	—	—
	4	13.2	12.3 (14.2)	21.1	13.0	6.5	1.7	0.76	0.62	—	—
	5	13.1	14.2 (14.5)	21.8	14.7	8.9	3.3	1.3	0.57	0.64	—

<sup>a</sup> Rate constant in parentheses is determined from the limiting slope of a semilog plot of ion abundance versus reaction time.

specific site in the molecule. Since these molecules possess several labile hydrogens, the MH<sup>+</sup>-d<sub>1</sub> species is most likely comprised of a distribution of species labeled with deuterium at different sites. The calculated k<sub>1</sub> rate constant realistically represents the sum of the rate constants for each individual d<sub>1</sub> species and gives the total rate for reaction at all sites. It is therefore important not to over interpret the rates obtained for sequential processes.

**Reactions with CD<sub>3</sub>OD.** With a proton affinity of 181.9 kcal/mol,<sup>28</sup> CD<sub>3</sub>OD is 15.4 kcal/mol more basic than D<sub>2</sub>O. The differences in proton affinities between CD<sub>3</sub>OD and the glycine oligomers range from 29.7 kcal/mol for Gly<sub>1</sub> to 49.9 kcal/mol for Gly<sub>5</sub>.<sup>24</sup> With few exceptions, CD<sub>3</sub>OD and D<sub>2</sub>O display similar reactivities toward the glycine oligomers (in terms of the number of exchanges and the pattern of rate constants). The small oligomers of Gly<sub>2</sub>H<sup>+</sup>, Gly<sub>3</sub>H<sup>+</sup>, and (Gly<sub>3</sub>-OMe)H<sup>+</sup> are observed to exchange all of their labile hydrogens with CD<sub>3</sub>OD. The oligomers larger than Gly<sub>3</sub> exchange at most two labile sites during the 20-s time period, displaying the same distinctive change in reactivity observed for larger molecules with D<sub>2</sub>O.

The two main differences between CD<sub>3</sub>OD and D<sub>2</sub>O are the observed rates of the reactions and the reactivity of Gly<sub>1</sub>H<sup>+</sup> with the reagents. Since CD<sub>3</sub>OD can only participate in a single deuterium exchange per reactive encounter, the reaction rate constants for the glycine oligomers with CD<sub>3</sub>OD are calculated using the sequential incorporation model discussed above. For Gly<sub>2</sub>H<sup>+</sup>, Gly<sub>3</sub>H<sup>+</sup>, and (Gly<sub>3</sub>-OMe)H<sup>+</sup>, the H/D exchanges are roughly 1.5 times faster with CD<sub>3</sub>OD than with D<sub>2</sub>O, and the exchange rate for Gly<sub>4</sub>H<sup>+</sup> is nearly five times faster with CD<sub>3</sub>OD (Table 1). (Gly<sub>4</sub>-OMe)H<sup>+</sup> and Gly<sub>5</sub>H<sup>+</sup> are still virtually unreactive with the reagent gas displaying exchange rates of (1–2)  $\times 10^{-12}$  cm<sup>3</sup> molecule<sup>-1</sup> s<sup>-1</sup>. The trends in the reactivity of CD<sub>3</sub>OD with the glycine oligomers demonstrate an upper limit to the difference in proton affinities of 50 kcal/mol, which is lower than the 61-kcal/mol limit for D<sub>2</sub>O.

The reactivity of Gly<sub>1</sub>H<sup>+</sup> displays the biggest difference between the two exchange gases. Where D<sub>2</sub>O is able to slowly exchange only one site on Gly<sub>1</sub>H<sup>+</sup>, CD<sub>3</sub>OD is observed to exchange all four labile hydrogens on the molecule. The results for Gly<sub>1</sub>H<sup>+</sup> in Table 1 are consistent with those of Gard *et al.*,<sup>22</sup> but are roughly twice as fast as their reported values. This difference could be attributed to the difficulty in accurately measuring gas pressures in the ICR cell. Our experiments utilize a Schulz-Phelps ionization gauge which is an integral component of the ICR call, calibrated against a capacitance manometer. Gard *et al.* use an externally located ion gauge and adjust their rate constants for back reactions with CH<sub>3</sub>OH impurities (up to 30%), during the exchange experiments.

**Reactions with CD<sub>3</sub>CO<sub>2</sub>D.** CD<sub>3</sub>CO<sub>2</sub>D is more efficient at promoting H/D exchange of the glycine oligomers. It has a higher proton affinity (190.2 kcal/mol)<sup>28</sup> compared to the reagents of D<sub>2</sub>O and CD<sub>3</sub>OD and demonstrates a smaller difference in proton affinities with the oligomers (21.4 kcal/mol for Gly<sub>1</sub> to 41.6 kcal/mol for Gly<sub>5</sub>). CD<sub>3</sub>CO<sub>2</sub>D is somewhat more reactive with the small oligomers of  $n \leq 3$  than CD<sub>3</sub>OD, since it is observed to exchange all the labile hydrogens of these oligomers during the 20-s reaction period (Table 1). The larger oligomers of Gly<sub>4</sub>H<sup>+</sup> and Gly<sub>5</sub>H<sup>+</sup> exchange several, but not all, of their labile hydrogens with CD<sub>3</sub>CO<sub>2</sub>D. As with the results of the two previous reagents, H/D exchange rates decrease with increasing proton affinity of the glycine oligomer. The overall rates of exchange are faster for CD<sub>3</sub>CO<sub>2</sub>D than for D<sub>2</sub>O and CD<sub>3</sub>OD, with the trend in rates following the proton affinity ordering D<sub>2</sub>O < CD<sub>3</sub>OD < CD<sub>3</sub>CO<sub>2</sub>D.

**Reactions with ND<sub>3</sub>.** ND<sub>3</sub> is the most basic exchange reagent used in this study. With a proton affinity of 204 kcal/mol,<sup>28</sup> ND<sub>3</sub> demonstrates the smallest differences in proton affinities with the glycine oligomers (ranging from 7.6 kcal/mol with Gly<sub>1</sub> to 27.8 kcal/mol with Gly<sub>5</sub>). ND<sub>3</sub> is the most efficient reagent studied for promoting H/D exchange of the glycine oligomers, as it exchanges every labile hydrogen site in each of the

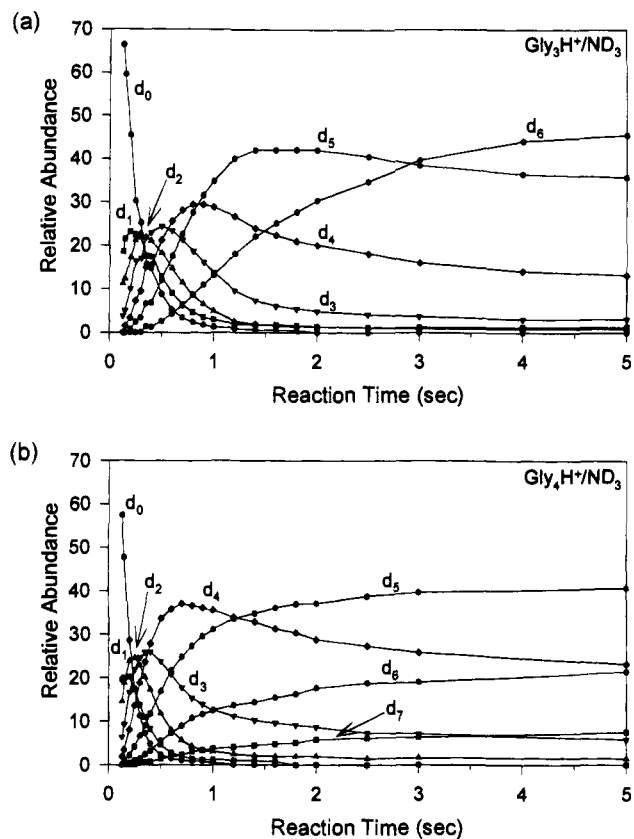


**Figure 4.** Time plots of the H/D exchange products of  $\text{Gly}_n\text{H}^+$  with  $\text{ND}_3$  ( $1.5 \times 10^{-7}$  Torr). (a)  $\text{Gly}_3\text{H}^+$  exchanges all six labile hydrogens rapidly. An equilibrium distribution of species is observed after 3–4 s due to a small presence of hydrogen impurities in the exchange gas (10 atom % hydrogen). (b)  $\text{Gly}_4\text{H}^+$  exchanges all seven labile hydrogens rapidly, but reaches an equilibrium distribution in which  $d_5$  is the most abundant species. The number of deuterium atoms incorporated into each species is indicated as  $d_n$ .

oligomers. In the small oligomers, the exchange rates are fast enough to achieve complete deuterium incorporation during a 7-s reaction period. A time plot for the H/D exchange of  $\text{Gly}_3\text{H}^+$  (containing six labile hydrogens) with  $\text{ND}_3$  is shown in Figure 4a. It is apparent that the  $\text{ND}_3$  reagent gas contains small amounts of  $\text{NHD}_2$  impurities, since an equilibrium distribution of incomplete exchange products is approached at long delay times. Analysis of the isotopic product distribution indicates the atom % deuterium in this system is 90%. The larger oligomers ( $n > 3$ ) display similar reactivity with  $\text{ND}_3$ , exchanging every labile site, but cannot complete the numerous exchanges on the molecule within the time frame of the experiments.  $\text{Gly}_4\text{H}^+$  is observed to undergo seven exchanges during the seven seconds of reaction with  $\text{ND}_3$ , but the reaction time plot in Figure 4b clearly demonstrates that the species with five deuteriums incorporated is the dominant species at this detection time.

$\text{ND}_3$  and  $\text{D}_2\text{O}$  are the only two reagent gases studied which have the potential to participate in multiple deuterium exchanges. Experiments were also performed to explore the possibility of multiple exchanges for  $\text{ND}_3$  in a single-collision event. Figure 5a shows the results of reacting  $\text{Gly}_3\text{H}^+$  with  $\text{ND}_3$  for 1 s. The  $\text{ND}_3$  pressure in this experiment was reduced from that in Figure 4a to observe a wider range of species at the 1-s detection time. Five deuteriums are incorporated into the oligomer during this time period. If the  $d_1$  species ( $m/z = 191$ , resulting from one exchange) is continuously ejected during the reaction, the yield of higher mass ions is diminished but not inhibited (Figure 5b). Comparing the product ion intensities of the two spectra

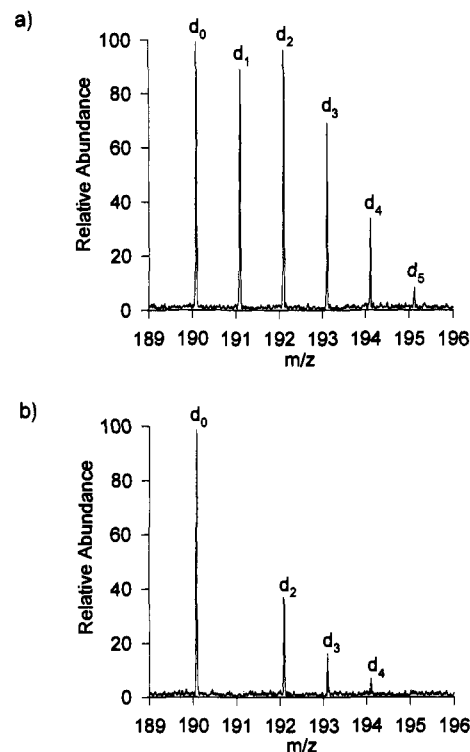


**Figure 5.** (a) H/D exchange products of  $\text{Gly}_3\text{H}^+$  with  $\text{ND}_3$  ( $5.0 \times 10^{-8}$  Torr) after 1 s. (b) Continuous ejection of the  $d_1$  ( $m/z = 191$ ) species during the reaction diminishes the amount of higher mass exchange products, but does not inhibit their formation.  $\text{ND}_3$  partakes in multiple exchanges during a single-collision event with  $\text{Gly}_3\text{H}^+$  22% of the time.

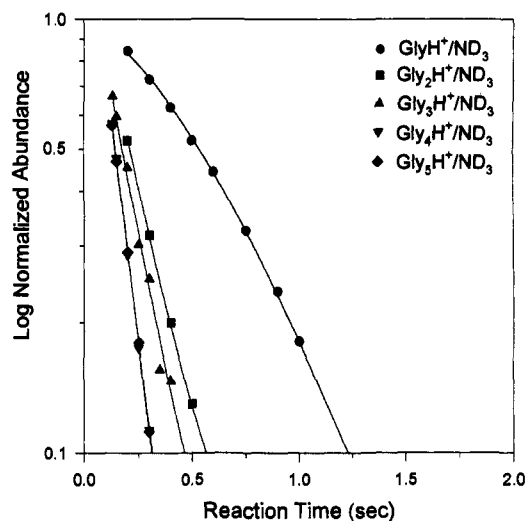


**Figure 6.** Semilog plots of ion abundance versus reaction time for  $\text{Gly}_n\text{H}^+$  with  $\text{ND}_3$ . Reaction rate constants for the first exchange are extracted from the limiting slope of each plot. H/D exchange rates increase with oligomer length. Curvature in the  $\text{Gly}_1\text{H}^+$  slope at short delays indicates a vibrationally and translationally hot population with decreases reactivity, which rapidly cools.

indicates that  $\text{ND}_3$  partakes in multiple exchanges during a single-collision event 22% of the time. Similar experiments with  $\text{Gly}_2\text{H}^+$  indicated that multiple exchanges occur 28% of the time.

Semilog plots of the H/D exchange data for  $\text{Gly}_n\text{H}^+$  ( $n = 1-5$ ) reacting with  $\text{ND}_3$  are shown in Figure 6. Disappearance rate constants ( $k_1$ ) are  $3.4 \times 10^{-10}$ ,  $7.4 \times 10^{-10}$ ,  $1.0 \times 10^{-9}$ ,  $1.4 \times 10^{-9}$ , and  $1.4 \times 10^{-9} \text{ cm}^3 \text{ molecule}^{-1} \text{ s}^{-1}$  for  $\text{Gly}_1\text{H}^+$  to  $\text{Gly}_5\text{H}^+$ , respectively. As with the results for  $\text{D}_2\text{O}$ , these calculated “first” rate constants give the total rate for reaction

at all labile sites in the molecule. Additionally, since  $\text{ND}_3$  partakes in multiple exchanges, these rate constants include contributions from processes which produce the  $\text{MH}^+-d_1$ ,  $-d_2$ , and  $-d_3$  species.

Determination of the subsequent reaction rate constants for the glycine oligomers with  $\text{ND}_3$  is more difficult than for  $\text{D}_2\text{O}$ ,  $\text{CD}_3\text{OD}$ , and  $\text{CD}_3\text{CO}_2\text{D}$ . A model using only sequential incorporation of deuterium (such as that  $\text{D}_2\text{O}$ ) neglects the contributions of roughly a quarter of the reactions which proceed by multiple exchanges. As a result, rate constants calculated from a sequential model will be in error. A product which incorporates three deuteriums will require three exchanges during the specified period using the sequential model, yet more realistically may be formed by multiple exchanges in a smaller number of reaction events. The calculated H/D exchange rate constants for the glycine oligomers with  $\text{ND}_3$  using a simple sequential model are listed in Table 1. Although careful selective ion ejection experiments can yield more information, the kinetic data themselves are insufficient to extract all of the rate constants in this system. Only the "first" exchange rate of  $\text{Gly}_n\text{H}^+$  can be determined with any accuracy from semilog plots of the experimental data, with the rate reflecting reactions by single and multiple exchange processes.

**Off-Resonance Excitation during H/D Exchange.** It is of interest to investigate the effects of increased translational and vibrational energy on the rates and extent of H/D exchange. This is of particular interest in systems where exchange is slow or not observed. Off-resonance excitation<sup>34</sup> was used to collisionally activate several oligomers during H/D exchange with  $\text{D}_2\text{O}$  and  $\text{CD}_3\text{CO}_2\text{D}$  reagent gases. In the off-resonance excitation experiments, rf excitation is applied at a frequency slightly different from the cyclotron frequency of the ion to be translationally excited. This causes the ion energy to oscillate with time, with an average given by eq 3, where  $q$  is the charge

$$\langle E_{\text{ion.cm}} \rangle = \frac{m_{\text{gas}}}{m_{\text{gas}} + m_{\text{ion}}} \left[ \frac{q^2 E_0^2}{4m_{\text{ion}}(\omega - \omega_c)^2} \right] \quad (3)$$

of the ion,  $E_0$  is the 0-peak amplitude of the applied electric field, and  $(\omega - \omega_c)$  is the difference between the applied excitation frequency and natural cyclotron frequency of the ion. For all examples in this article, excitation was applied on the high-frequency or low-mass side of the ion to avoid exciting higher mass exchange products whose cyclotron frequencies are lower and thus further off resonance in accordance with eq 3. Vibrational excitation of the ions results from sequential multiple collisions (at elevated translational energies) with appropriate gases.  $\text{D}_2\text{O}$  and  $\text{CD}_3\text{CO}_2\text{D}$  serve both as exchange and collision gases. The conversion of translational energy into vibrational energy in low-energy collisions is predicted to be very efficient for molecules of this size.<sup>38</sup> Excitation levels were adjusted to maximize translational and vibrational excitation, while promoting a minimum amount of collisional dissociation.

The results for  $\text{Gly}_4\text{H}^+$  reacting with  $\text{CD}_3\text{CO}_2\text{D}$  are shown in Figure 7. Exchange reactions were monitored over a period of seconds with and without activation at an average center of mass collision energy of 0.18 eV. During the first 1.5 s of the reaction, the H/D exchange rates are slower with off-resonance excitation applied. A decrease in the reaction rate constant with increasing translational energy is often characteristic of exothermic ion-molecule reactions. When  $\text{Gly}_3\text{H}^+$  is translationally and vibrationally excited using  $\text{D}_2\text{O}$ , the H/D exchange rates also appear to decrease slightly. Under thermal conditions,

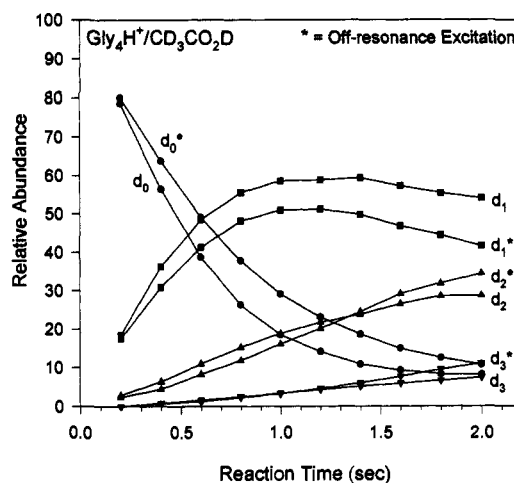


**Figure 7.** H/D exchange of  $\text{Gly}_4\text{H}^+$  with  $\text{CD}_3\text{CO}_2\text{D}$  ( $7.6 \times 10^{-8}$  Torr), with and without off-resonance collisional activation. Translational and vibrational excitation leads to a lower rate of exchange for the excited species ( $d_0^*$ ). Species labeled as  $d_n^*$  are exchange products of excited  $\text{Gly}_4\text{H}^+$ .

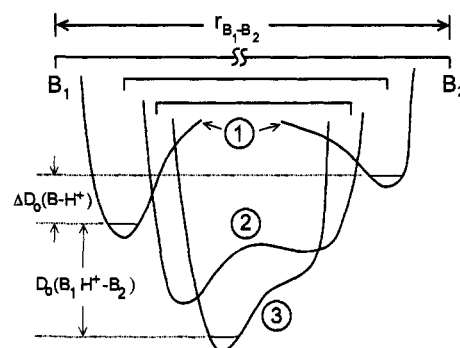


**Figure 8.** Potential energy surfaces for proton motion between  $B_1$  and  $B_2$  for several values of the separation of the basic sites in  $B_1$  and  $B_2$ . At large separations, curve 1, the surface approximates that of the isolated systems, and the difference in well depths is approximately equal to the difference in proton affinities  $\Delta D_0(\text{B}-\text{H}^+)$ . As the reactants approach, the barrier to proton transfer is reduced (curve 2) and the total energy of the system is lowered. At equilibrium (curve 3), the energy decrease equals the hydrogen bond energy  $D_0(\text{B}_1\text{H}^+-\text{B}_2)$ .

$\text{Gly}_4\text{H}^+$  only undergoes one slow exchange with  $\text{D}_2\text{O}$  (Figure 1d). Collisional activation of  $\text{Gly}_4\text{H}^+$  does not enhance reactivity. In fact, high excitation levels caused extensive collisional dissociation during the reaction period. The excitation causes no noticeable effect on the rate or extent of H/D exchange in  $\text{Gly}_4\text{H}^+$ .

## Discussion

Several recent studies report a correlation between the extent of H/D exchange observed for a molecule and the absolute difference in proton affinities between the molecule and the exchange reagent.<sup>14,22,23</sup> Some researchers have reported that H/D exchange cannot occur between species which differ by more than 20 kcal/mol,<sup>14</sup> while others have observed exchange between species which differ by more than 50 kcal/mol.<sup>23</sup>

Isotopic hydrogen exchange processes are generally initiated by the formation of a strong hydrogen bond between the reactant ion (designated  $\text{B}_1\text{H}^+$ , assuming a protonated species) and the neutral exchange reagent (designated  $\text{B}_2$ ). The energetics of this process can be discussed with reference to the potential energy surface in Figure 8, in which the variation in energy with proton position is shown for several values of the  $\text{B}_1-\text{B}_2$  separation (determined by the internuclear spacing of the sites

(38) Marzluff, E. M.; Campbell, S.; Rodgers, M. T.; Beauchamp, J. L. *J. Am. Chem. Soc.* **1994**, *116*, 6947.

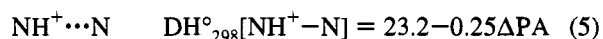
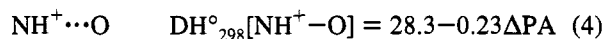


**Table 2.** Calculated and Experimental Proton Affinities<sup>a</sup> for the Glycine Oligomers

Gly <sub>n</sub> oligomer	PA (calculated)				ΔPA (folded-open)		PA (experimental)		
	AM1		PM3		AM1	PM3	Fenselau <sup>b</sup>	Lebrilla <sup>c</sup>	Cassady <sup>d</sup>
	folded	open	folded	open					
Gly <sub>1</sub>	— <sup>e</sup>	200.1	— <sup>e</sup>	200.5	— <sup>e</sup>	— <sup>e</sup>	211.6	210.1	208.3
Gly <sub>2</sub>	210.6	205.1	209.4	206.0	5.15	3.4	219.1	218.5	217.4
Gly <sub>3</sub>	219.8	206.6	216.3	206.5	13.2	9.8	223.1	219.8	220.6
Gly <sub>4</sub>	227.6	207.1	222.0	208.6	20.5	13.4	227.2	219.8	226.0
Gly <sub>5</sub>	235.8	209.0	230.1	207.0	26.8	23.1	231.8	221.7	226.3

<sup>a</sup> Proton affinities in kcal/mol. <sup>b</sup> Reference 24. <sup>c</sup> Reference 25. <sup>d</sup> Reference 26. <sup>e</sup> (—) Gly<sub>1</sub> does not exhibit folding.

of protonation). Figure 8 is adapted from *ab initio* calculations for the system NH<sub>4</sub><sup>+</sup>⋯OH<sub>2</sub>.<sup>39</sup> At large separations, the well depths approach the limiting values associated with the proton affinities of the isolated bases. As the separation decreases, the total energy of the system decreases to reflect the strength of the hydrogen bond, DH<sup>o</sup><sub>298</sub>[B<sub>1</sub>H<sup>+</sup>—B<sub>2</sub>]. Depending on B<sub>1</sub> and B<sub>2</sub> the potential surface may exhibit either single or double minima. If the energy released by formation of a strong hydrogen bond is sufficient to allow the proton motion to sample regions of the potential energy surface in which it approaches within normal bonding distance to B<sub>2</sub>, then it is highly probable that this motion can couple with other degrees of freedom and result in facile isotopic hydrogen exchange. Meot-Ner has investigated a large series of complexes in an attempt to quantitate the strengths of typical strong hydrogen bonds.<sup>18</sup> Equations 4 and 5 can be used to determine the hydrogen bond strengths in a dimer containing a protonated amine and an oxygen or nitrogen donor base, respectively, where ΔPA is the difference in proton affinities of B<sub>1</sub> and B<sub>2</sub>. If we consider only basic sites involving the heteroatoms N and O and avoid systems where steric effects constrain the approach of the two basic centers, then it is reasonable to assume that the barrier to proton transfer will be either small



or non-existent (Figure 8). We can then take the differences in proton affinities of the two bases as an upper limit to the hydrogen bond strength required to permit facile isotopic hydrogen exchange (i.e., DH<sup>o</sup><sub>298</sub>[B<sub>1</sub>H<sup>+</sup>—B<sub>2</sub>] = ΔPA). Equations 4 and 5 indicate that this occurs at proton affinity differences of 23 and 19 kcal/mol, respectively, for oxygen and nitrogen bases. These considerations are consistent with the observations that H/D exchange is often not observed between simple species whose proton affinity difference exceeds approximately 20 kcal/mol. In applying it to the present study, this simple mechanistic picture can be used to explain the H/D exchange of species like ND<sub>3</sub> with Gly<sub>1</sub>H<sup>+</sup> or Gly<sub>2</sub>H<sup>+</sup>, whose proton affinity differences are less than 20 kcal/mol, and where folding does not lead to significant stabilization from intramolecular hydrogen bonding in B<sub>1</sub>H<sup>+</sup>. Unfortunately, the difference in proton affinities between most of the peptides and reagent gases is larger than 20 kcal/mol and this picture does not suffice to explain most of our observations.

Our experimental results for the protonated glycine oligomers indicate H/D exchange can occur between molecules with large differences in proton affinities. D<sub>2</sub>O, with a proton affinity of 166.5 kcal/mol, undergoes facile H/D exchange with Gly<sub>3</sub>H<sup>+</sup> (PA = 223.1 kcal/mol) but is unreactive toward Gly<sub>4</sub>H<sup>+</sup> (PA = 227.2 kcal/mol). This places the upper limit to reactivity

between 57 and 61 kcal/mol. Using the same analysis for CD<sub>3</sub>-OD (PA = 181.9 kcal/mol) reacting with Gly<sub>4</sub>H<sup>+</sup> and Gly<sub>5</sub>H<sup>+</sup> (PA = 231.8 kcal/mol), the upper limit changes to 45–50 kcal/mol. Additionally, Gly<sub>2</sub>H<sup>+</sup> (PA = 219.1 kcal/mol) reacts with D<sub>2</sub>O, whereas Gly<sub>1</sub>H<sup>+</sup> (PA = 211.6 kcal/mol) is mostly unreactive. It is clear from these results that the propensity of a specific system to exhibit isotopic hydrogen exchange is dependent on factors other than differences in proton affinities.

To understand the present results, it is useful to have some notion of the potential energy surfaces for H/D exchange with these supposedly "simple" model systems. High-quality *ab initio* calculations are not feasible for systems as large as these, however. For this reason, we resort to the use of AM1 and PM3 semiempirical calculations to provide a semiquantitative assessment of the energetics of postulated reaction intermediates and to construct reaction coordinate diagrams for different proposed mechanisms.

**Semiempirical Calculations.** Semiempirical calculations were performed using Hyperchem<sup>35</sup> computational software to obtain model structures and energetics for the protonated glycine oligomers and reagent exchange gases. The calculations were performed using both the AM1 and the PM3 methods. The proton affinities are found from the calculated heats of formation of the geometry optimized neutral and protonated molecules. Dewar and coworkers<sup>30</sup> have provided a comprehensive comparison of calculated and experimental heats of formations for both neutrals and ions using the AM1 method. The PM3 method has similarly been evaluated.<sup>31</sup> Using the AM1 method, errors in the calculated heats of formation of protonated species are comparable with those in the neutral precursors. With the PM3 method, the average difference between the predicted heats of formation and experimental values for 657 compounds was 7.8 kcal/mol, and for 106 hypervalent compounds, 13.6 kcal/mol. The PM3 method differs from the AM1 method only in the values of the parameters. In the critical area of modeling the strengths and energies of hydrogen bonds, the PM3 method is preferred. Numerous investigations conclude that AM1 geometries are in poor agreement with *ab initio* calculations, whereas PM3 gives geometries similar to *ab initio* structural results.<sup>40</sup> The main limitations in the PM3 method are the underestimation of hydrogen bond lengths by 0.1–0.2 Å for some systems and the underestimation of reliable experimental hydrogen bond strengths by approximately 1–2 kcal/mol.<sup>40</sup>

Table 2 summarizes the calculated and experimental thermochemical properties for the glycine oligomers considered in the present study. While agreement in most instances is fairly good, there are some obvious problems. Most importantly, the predicted proton affinity of glycine is 200.1 and 200.6 kcal/mol by the AM1 and PM3 methods, respectively, compared to the experimental value of 211.6 kcal/mol.<sup>24</sup> Calculations for ammonia indicate the error is in the opposite direction with

(39) Jaroszewski, L.; Lesyng, B.; Tanner, J. J.; McCammon, J. A. *Chem. Phys. Lett.* **1990**, *175*, 282.

(40) See, for example: (a) Zheng, Y.; Merz, K. M. *J. Comp. Chem.* **1992**, *13*, 1151. (b) Jurema, M. W.; Shields, G. C. *J. Comp. Chem.* **1993**, *14*, 89.

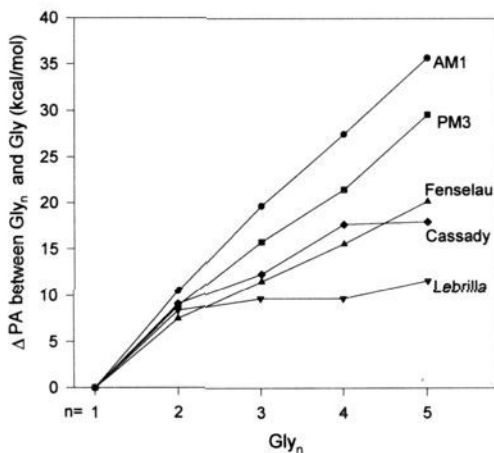


**Figure 9.** Comparison of the experimental and calculated proton affinities of the glycine oligomers relative to Gly<sub>1</sub>. AM1 calculations appear to overestimate the proton affinity differences between the oligomers, whereas experimental results by Lebrilla<sup>25</sup> appear to underestimate the differences in large oligomers. Fenselau<sup>24</sup> and Cassady<sup>26</sup> predict similar trends in proton affinities using different experimental techniques. The PM3 method gives better agreement with experimental results than does AM1.

predicted values of 207.9 and 209.2 kcal/mol with AM1 and PM3 methods, respectively, being higher than the experimental value of 204.0 kcal/mol. Hence proton transfer from NH<sub>4</sub><sup>+</sup> to glycine is predicted to be endothermic by approximately 8 kcal/mol when it is exothermic by nearly the same amount. ICR experiments which probe the reverse reaction give no evidence for proton transfer from Gly<sub>1</sub>H<sup>+</sup> to NH<sub>3</sub>.<sup>26</sup>

As a starting point for considering the mechanism of exchange, structures were calculated for the protonated glycine oligomers. In all cases the proton is preferentially bound to the N-terminus and the peptide folds up to solvate the charge site, mainly by forming hydrogen bonds to carbonyl oxygens. The starting point for each structure involves a  $\beta$ -sheet configuration. For Gly<sub>n</sub>H<sup>+</sup> ( $n = 2-4$ ) in the folded form, the N-terminus glycine prefers a cis amide bond in the most stable structure. With Gly<sub>5</sub>H<sup>+</sup>, structures with the N-terminus glycine in both the cis and trans forms were of comparable stability.

Calculated proton affinities<sup>41</sup> of the glycine oligomers are summarized in Table 2 and compared with available experimental results.<sup>42</sup> The comparison is shown graphically in Figure 9. AM1 calculations are known to predict hydrogen bond strengths which are somewhat higher than experimental values, whereas the PM3 method gives somewhat better agreement.<sup>40</sup> The results in Figure 9 suggest the same trends, with PM3 giving better results. Both the kinetic and bracketing methods of determining proton affinities have been subjected to critical analysis which will not be repeated here.<sup>43</sup> The variance in experimental results from three different laboratories (shown in Figure 9) reflects some of the difficulties with these experimental methodologies. Additionally, the semiempirical calculations do not directly take into account heat capacities of

(41) Neutral heats of formation were evaluated with the glycine oligomers in an extended  $\beta$ -sheet configuration. Folded configurations did not have significantly different energies.

(42) All experimental results are reported relative to the proton affinity of NH<sub>3</sub> as 204.0 kcal/mol.<sup>28</sup> Values which were reported in the literature using the recent scale by Meot-Ner (Meot-Ner, M.; Sieck, L. W. *J. Am. Chem. Soc.* **1991**, *113*, 4448) have been adjusted using their NIST gas phase basicities<sup>28</sup> and adding the appropriate  $T\Delta S$  terms estimated by each investigator.

(43) (a) Bliznyuk, A. A.; Schaeffer, H. F.; Amster, I. J. *J. Am. Chem. Soc.* **1993**, *115*, 5149. (b) Bojesen, G.; Breindahl, T. *J. Chem. Soc., Perkin Trans. 2* **1994**, 1030.

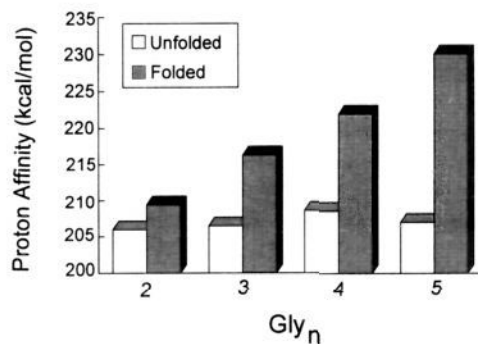


**Figure 10.** Calculated proton affinities for linear (unfolded) and hydrogen-bonded (folded) glycine oligomers using the PM3 method. Proton affinities of the unfolded molecules are relatively constant. The majority of increase in the proton affinity of the oligomers comes from folding to solvate the charge center.

these molecules, which possess many low-frequency vibrational modes, to calculate true 298 K heats of formation. With this in mind, we consider that the agreement indicated in Figure 9 is reasonable and we have selected the PM3 calculations for further consideration.

It is instructive to estimate the contribution which folding makes to the stability of the protonated glycine oligomers. Separate calculations were carried out for the protonated species in the extended  $\beta$ -sheet and in the compact hydrogen-bonded configurations. Results of these calculations are given in Table 2. Whereas the proton affinities of the compact, hydrogen-bonded oligomers display a smooth increase from Gly<sub>1</sub> to Gly<sub>5</sub>, the proton affinities of the linear oligomers stay relatively constant. Figure 10 indicates that the extended form experiences a sizable increase in proton affinity only in proceeding from Gly<sub>1</sub> to Gly<sub>2</sub>. The regular increase in proton affinity predicted and observed for the glycine oligomers comes mainly from the folding contribution to solvate the charge site. In the case of Gly<sub>5</sub>, this accounts for 83% of the increase relative to glycine.

**Do Glycine Oligomers Form Zwitterions (Salt Bridges) in the Gas Phase?** The unusual change in reactivity observed for Gly<sub>3</sub>H<sup>+</sup> and Gly<sub>4</sub>H<sup>+</sup> with D<sub>2</sub>O caused us to consider the possibility of forming zwitterions in the gas phase. Peptides are known to exist in solution in their zwitterionic forms. To form a zwitterion in the gas phase is energetically unfavorable without solvent stabilization.<sup>44</sup> However, the molecular structures obtained from semiempirical calculations indicated that the addition of one glycine unit to the Gly<sub>3</sub> polymer is enough to allow the peptide ends to interact. An intriguing possibility for the gas-phase structure of Gly<sub>4</sub>H<sup>+</sup> is a zwitterion in which the ionic ends can approach each other, forming a salt bridge, and allow for the resulting Coulombic attraction to compensate for the nominally endothermic process of forming an isolated ion pair.<sup>45</sup> The labile proton would be attached to a basic amide oxygen. Such a species might be feasible for Gly<sub>4</sub>H<sup>+</sup> and not Gly<sub>3</sub>H<sup>+</sup>.

Consider reaction I for glycine, in which an isolated ion pair is formed. This is predicted by PM3 calculations to be endothermic by 141.6 kcal/mol. From gas-phase proton affinity and acidity measurements, the experimental value is endothermic by 130.0 kcal/mol.<sup>28</sup> Most of the error in the calculated value



(44) Locke, M. J.; McIver, R. T., Jr. *J. Am. Chem. Soc.* **1983**, *105*, 4226.

(45) It has been shown that acid-base complexes can form ion pairs in the gas phase. See, for example: Legon, A. C. *Chem. Soc. Rev.* **1993**, *22*, 153.

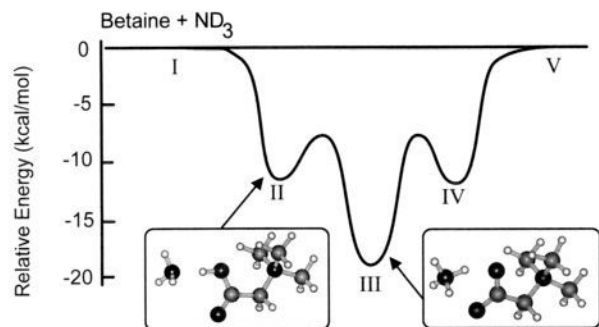


**Figure 11.** Potential energy surface for the H/D exchange of betaine with  $\text{ND}_3$  via a salt bridge mechanism. A strong hydrogen bond is formed as the reagent base approaches the carboxylic acid group. Proton transfer to  $\text{ND}_3$  forming a stable salt bridge is highly favorable and results in facile exchange of the carboxylate.

is in the proton affinity calculation as noted above. Calculations were first performed to determine if the longer, more flexible chain of  $\text{Gly}_5$  neutral could possibly form a stable salt bridge in the gas phase. Structures which possessed neutral termini were always found to be lower in energy. The most stable  $\text{Gly}_5$  zwitterion was estimated to be 20 kcal/mol less stable than the neutral  $\beta$ -sheet configuration.

Addition of a proton to the salt bridge form of neutral  $\text{Gly}_5$  occurs on the amide oxygen adjacent to the C-terminus, to give the salt bridge shown in structure 2. PM3 results indicate that this species is 17.4 kcal/mol less stable than the folded  $\text{Gly}_5\text{H}^+$  (structure 3). Similar calculations for  $\text{Gly}_4\text{H}^+$  and  $\text{Gly}_3\text{H}^+$

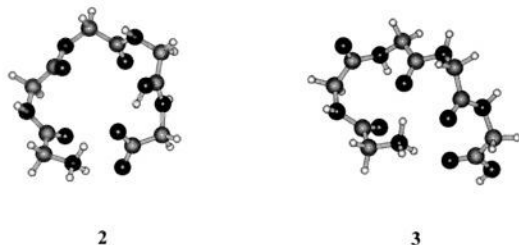


exhibit increasingly less stable salt bridge forms relative to the folded structures, protonated on the N-terminus. Experimental results with the methyl esters support the theoretical calculations. The H/D exchange of  $(\text{Gly}_4\text{-OME})\text{H}^+$  with  $\text{D}_2\text{O}$  displays the same results as  $\text{Gly}_4\text{H}^+$  with only one deuterium incorporated. If  $\text{Gly}_4\text{H}^+$  had been a salt bridge, methylation of the C-terminus should have disrupted the structure and varied the observed exchange pattern.

**Mechanism of Exchange for Betaine.** Before considering exchange mechanisms for the protonated glycine oligomers, it is of interest to reflect on the mechanism by which our probe molecule, betaine (1), exchanges its single labile hydrogen with the reagents used in this study. Betaine is unusual in that with the quaternary nitrogen, the molecule does not possess a labile proton. Even so, facile exchange occurs with  $\text{ND}_3$ ,  $\text{CD}_3\text{CO}_2\text{D}$ , and  $\text{CD}_3\text{OD}$ , as shown by the rates in Table 1.  $\text{D}_2\text{O}$  is two orders of magnitude slower. Betaine represents a model system for better understanding what might occur in exchange of the carboxyl hydrogen in the protonated glycine oligomers.

Calculations at the PM3 level indicate that  $\text{NH}_3$  forms a relatively strong hydrogen bond to betaine (12.6 kcal/mol). Furthermore, proton transfer to  $\text{NH}_3$ , forming a salt bridge, is

actually exothermic by 18 kcal/mol (Scheme 1)! The reaction

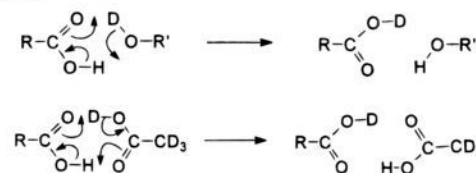
#### Scheme 1



coordinate diagram is shown in Figure 11 along with the structures of the exchange intermediates. Similar calculations for  $\text{CH}_3\text{CO}_2\text{H}$  indicate that salt bridge formation with betaine is feasible since the hydrogen-bonded intermediate is lower in energy by 12.0 kcal/mol than the separated reagents, and proton transfer from betaine to acetic acid is slightly exothermic (0.1 kcal/mol). Salt bridge formation is not favorable with  $\text{D}_2\text{O}$  and  $\text{CD}_3\text{OD}$ , presumably due to the lower proton affinities compared to  $\text{NH}_3$ .

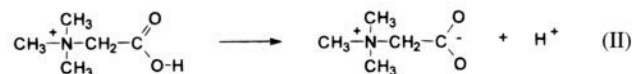
It is more difficult to evaluate the possibility of multicenter "flip-flop" exchange intermediates such as those shown in Scheme 2. The barriers for these processes may be high

#### Scheme 2



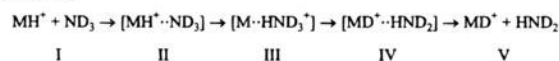
compared to the chemical activation available from complex formation. A possible exception is acetic acid, where barriers for exchange in symmetric hydrogen-bonded acid dimers are known to be 10–12 kcal/mol.<sup>46</sup>

The results with betaine are perhaps not surprising if one considers the gas-phase acidity of the ion ( $\Delta H$  for reaction II). PM3 calculations yield a value of 241.3 kcal/mol, which suggests that it should be possible to deprotonate betaine with strongly basic neutral species. For comparison, the acidity of glycine is 341.6 kcal/mol.<sup>28</sup> The nearby positive charge center significantly stabilizes the carboxylate anion in deprotonated betaine.<sup>47</sup>



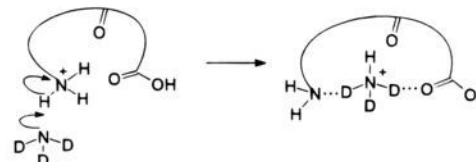
**Mechanisms of Exchange for  $\text{ND}_3$ .** A reaction intermediate comprising a chemically activated hydrogen-bonded complex is initially invoked (Scheme 3). From experimental proton

#### Scheme 3



affinities, it is predicted that proton transfer from a glycine oligomer to an ammonia molecule should be moderately unfavorable. We propose that the mechanism of facile H/D exchange for the glycine oligomers with  $\text{ND}_3$  involves molecular choreography in which an endothermic proton transfer is rendered energetically feasible by solvation of the resultant ammonium ion (Scheme 4). Solvation of this ion by the

#### Scheme 4



(46) Shida, N.; Barbara, P. F.; Almlof, J. *J. Chem. Phys.* **1991**, *94*, 3633.

(47) The effects of nearby charges on the energetics of proton transfer reactions have been considered by: Sanhueza, J. E.; Tapia, O. *J. Mol. Struct.* **1982**, *89*, 131.

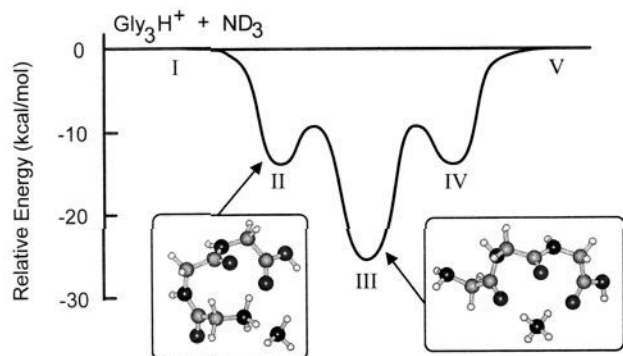


**Figure 12.** Potential energy surface for the H/D exchange of  $\text{Gly}_3\text{H}^+$  with  $\text{ND}_3$  via an onium ion mechanism. Proton transfer from the N-terminus to  $\text{ND}_3$  is accompanied by simultaneous solvation of the ammonium ion by the carbonyl oxygens of the peptide.

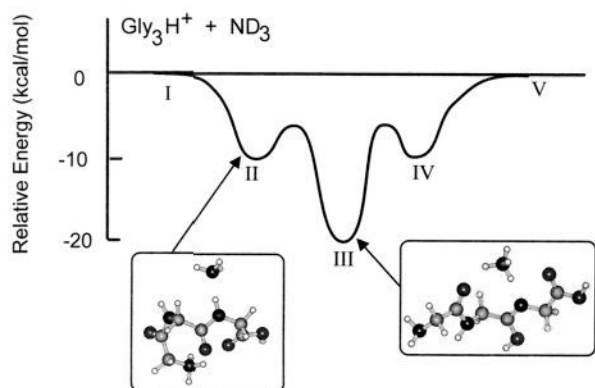


**Figure 13.** Potential energy surface for the H/D exchange of amide hydrogens of  $\text{Gly}_3\text{H}^+$  with  $\text{ND}_3$  via a tautomer mechanism. Proton transfer from the N-terminus to an amide carbonyl occurs in concert with transfer of the amide proton to ammonia.

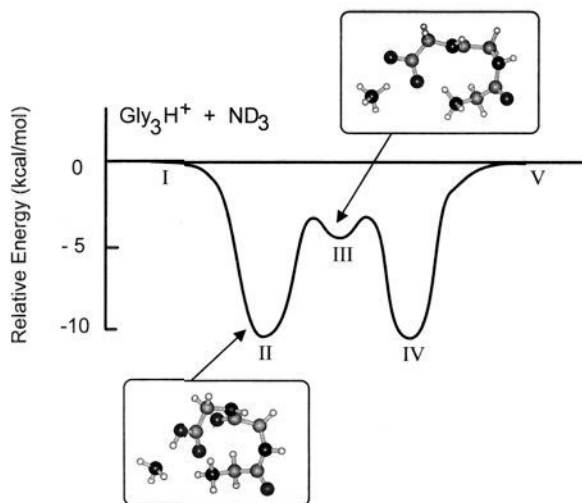


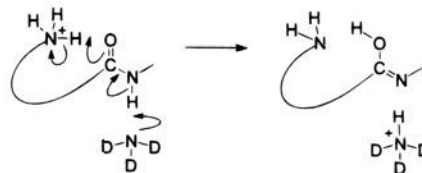
**Figure 14.** Potential energy surface for the H/D exchange of the C-terminus of  $\text{Gly}_3\text{H}^+$  with  $\text{ND}_3$  via a salt bridge mechanism. Proton transfer from the C-terminus to  $\text{ND}_3$  and formation of a salt bridge structure is facilitated by the stabilizing effect of the nearby positively charged N-terminus.

oligomer compensates for the loss of folding stabilization in the parent species (I). PM3 calculations show the onium ion mechanism for H/D exchange is especially favorable for ammonia, as the solvated ammonium ion complex (species III) with  $\text{Gly}_3$ ,  $\text{Gly}_4$ , and  $\text{Gly}_5$  is 25.1, 23.9, and 19.3 kcal/mol more stable than the separated reactants, respectively. As a result,

$\text{ND}_3$  is a highly effective reagent for promoting H/D exchange with these oligomers. The calculated reaction coordinate diagram for the exchange of  $\text{Gly}_3\text{H}^+$  with  $\text{ND}_3$  is shown in Figure 12, with the intermediates numbered as in Scheme 3. It should be kept in mind that we have only estimated the energetics of reactants, products, and stable intermediates in constructing these reaction coordinate diagrams. The barriers which separate the minima remain unknown except that they must be consistent with the observed reactivity. It should be obvious from the reaction coordinate diagram of Figure 12 that multiple exchanges are possible with  $\text{ND}_3$ , since the intermediates can rattle around in the several wells before dissociating to products.

H/D exchange of the amide and carboxylic hydrogens in the glycine oligomers by  $\text{ND}_3$  requires further considerations. The energetics of several possible mechanisms were evaluated with semiempirical calculations. Only one viable pathway was discerned which is nearly as energetically favorable as the exchange of the N-terminus hydrogens. The mechanism proposed for exchanging the amide hydrogen involves proton transfer from the N-terminus to the amide carbonyl in concert with transfer of the amide proton to ammonia to form an ammonium ion solvated by the tautomerized peptide (Scheme 5). The reaction coordinate diagram for the amide hydrogen

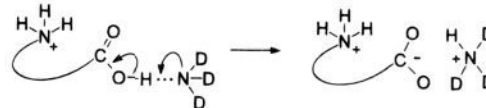
#### Scheme 5



exchange of  $\text{Gly}_3\text{H}^+$  with  $\text{ND}_3$  is shown in Figure 13. The tautomerized intermediate is only 5.2 kcal/mol less stable than the onium ion intermediate in Figure 12, and is 19.9 kcal/mol below the energy of the reactants. We will refer to this process as the tautomer mechanism.

An intriguing possibility for exchange of the carboxylate hydrogen invokes salt bridge formation. In analogy with the exchange process proposed above for betaine, this process involves proton transfer from the C-terminus to ammonia with concomitant stabilization of the carboxylate anion by the protonated N-terminus (Scheme 6). PM3 calculations suggest

#### Scheme 6



favorable energetics for this process as shown in Figure 14. The salt bridge structure involving the C-terminus carboxylic acid is a local minimum on the reaction coordinate diagram, but is only 4 kcal/mol lower in energy than the reactants. This species will have a tendency to collapse to the significantly more stable onium ion (Figure 12) by transferring a proton from the N-terminus to the carboxylate anion, and the end result can be considered a degenerate tautomer mechanism. Even so, it appears to provide a viable pathway to eventually exchange the C-terminus hydrogen.

**Mechanism of Exchange for  $\text{D}_2\text{O}$ .** For  $\text{D}_2\text{O}$  to undergo H/D exchange with the glycine oligomers, a proton affinity difference of at least 45.1 kcal/mol (for  $\text{Gly}_1$ ) must be overcome. This effectively rules out exchange via simple hydrogen bond formation as in Figure 8, which is inefficient for proton affinity

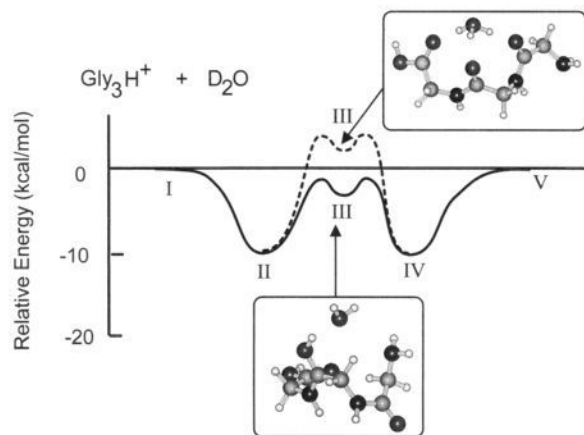
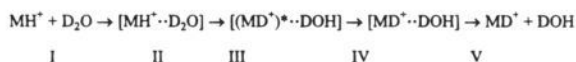


**Figure 15.** Potential energy surfaces for the H/D exchange of  $\text{Gly}_3\text{H}^+$  with  $\text{D}_2\text{O}$  via relay and onium ion mechanisms. Proton transfer to  $\text{H}_2\text{O}$  and formation of a hydronium ion intermediate (dashed line) is unfavorable due to the low proton affinity of  $\text{H}_2\text{O}$ . Instead, exchange occurs via a relay mechanism (solid line) in which a proton is shuttled by  $\text{D}_2\text{O}$  from the N-terminus to an amide carbonyl, leaving the charge site on the peptide.

differences greater than 20 kcal/mol. Additionally, exchange by means of a salt bridge mechanism is unlikely since calculations indicate this process is unfavorable for  $\text{H}_2\text{O}$ , due to the much lower proton affinity of  $\text{H}_2\text{O}$  compared to  $\text{NH}_3$ . Semiempirical PM3 calculations also indicate that H/D exchange by formation of a solvated hydronium ion complex with the glycine oligomers is energetically unfavorable. The proton affinity of  $\text{D}_2\text{O}$  is too low and the energy recovered by solvation of the hydronium ion is insufficient to overcome the endothermicity of proton transfer. The reaction coordinate diagram for the H/D exchange reaction of  $\text{Gly}_3\text{H}^+$  with  $\text{D}_2\text{O}$  by means of an onium ion mechanism is shown in Figure 15, with the intermediates labeled similarly to those of Scheme 3. Although the hydrogen-bonded complex of  $\text{Gly}_3\text{H}^+$  with  $\text{D}_2\text{O}$  is a local minimum, transfer of the proton to  $\text{D}_2\text{O}$  is unfavorable by 2.1 kcal/mol compared to the separated starting species.

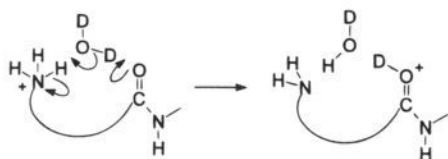
We propose a relay mechanism for facile H/D exchange of protonated peptides with  $\text{D}_2\text{O}$  in which a proton is shuttled from the site of protonation in the hydrogen-bonded complex onto  $\text{D}_2\text{O}$  in concert with the transfer of a deuteron from  $\text{D}_2\text{O}$  to a distant, slightly less basic site on the molecule (Schemes 7 and

#### Scheme 7



8). For the glycine oligomers, this corresponds to the labile

#### Scheme 8



charge being shuttled from the N-terminus nitrogen (species II) to a less basic amide oxygen (III). The reaction coordinate diagram calculated for the H/D exchange of  $\text{Gly}_3\text{H}^+$  with  $\text{D}_2\text{O}$  via the relay mechanism is shown in Figure 15, with the intermediates numbered as in Scheme 7. Deuteron transfer from the relay intermediate (III) back to the N-terminus nitrogen (IV) and dissociation to products completes the reaction process. The

relay mechanism makes proton transfer viable within a molecule using the chemical activation provided by hydrogen bonding.

Although it is possible for reactants to traverse the potential energy surface several times, it seems reasonable that the relay surface for  $\text{D}_2\text{O}$  is less conducive to multiple exchanges than the onium ion surface for  $\text{ND}_3$  in Figure 12. PM3 calculations were performed to identify if  $\text{ND}_3$  undergoes H/D exchange with the glycine oligomers via the relay mechanism. Calculations indicate that with  $\text{ND}_3$ , relay intermediates are energetically feasible but readily collapse to the more stable solvated ammonium ion (III, Figure 12).

**Differences in Reactivity between the Oligomers.** There are two unusual features observed in the reactivity of the glycine oligomers with the exchange reagents. The first is the lack of reactivity of  $\text{Gly}_1$  with  $\text{D}_2\text{O}$  while  $\text{Gly}_2$  exchanges all labile hydrogens. The second is the lack of reactivity of oligomers larger than  $\text{Gly}_3$  with  $\text{D}_2\text{O}$  and to a lesser extent  $\text{CD}_3\text{OD}$ .

Reactions of the oligomers with  $\text{D}_2\text{O}$  proceed via the relay mechanism. The mechanism makes viable reactions that are nominally endothermic by forming hydrogen bonds between  $\text{D}_2\text{O}$  and the exchange sites. For exchanges to occur, the energy gained by forming hydrogen bonds must be larger than the difference in the proton affinities of the exchange sites and the energy lost by opening the internally solvated structure.  $\text{Gly}_2\text{H}^+$  easily exchanges with  $\text{D}_2\text{O}$  via the relay mechanism since very little folding energy is lost by forming the intermediate (Figure 10), and the difference in proton affinity between the N-terminus nitrogen and the amide oxygen is small (8.1 kcal/mol).<sup>48</sup>  $\text{Gly}_1\text{H}^+$  cannot easily exchange with  $\text{D}_2\text{O}$  via the relay mechanism since the two sites for shuttling the proton are the N-terminus nitrogen and the acid carbonyl. The difference in proton affinities between these sites is calculated to be 13.4 kcal/mol, which is more than the amount recovered by forming a hydrogen-bonded intermediate. The one slow exchange observed for  $\text{Gly}_1\text{H}^+$  probably occurs at the acid hydroxyl, remote from the charge center via a salt bridge (analogous to Scheme 1) or by a multicenter exchange similar to Scheme 2. The energetics of the salt bridge formation should not be very different from those of betaine.

For  $\text{Gly}_3\text{H}^+$  and  $\text{Gly}_4\text{H}^+$  the difference in folding energies probably accounts for the observed difference in reactivity with  $\text{D}_2\text{O}$ . Molecular dynamics simulations<sup>49</sup> show that when  $\text{D}_2\text{O}$  hydrogen bonds to  $\text{Gly}_3\text{H}^+$ , the secondary structure of the molecule is disrupted in less than a picosecond at 300 K. The rupturing of the internal hydrogen bonds exposes labile hydrogen sites and facilitates exchange by the relay mechanism. The energy recovered by forming the exchange intermediate compensates for the loss in intramolecular folding energy. The proton affinity of  $\text{Gly}_4$  is larger than that of  $\text{Gly}_3$  due to more extensive solvation of the charge site. This effectively increases the disparity in proton affinities between the solvated N-terminus and amide oxygens in the molecule, thereby reducing the effectiveness of the relay mechanism for exchange. Molecular dynamics simulations show that the more extensive intramolecular hydrogen bonding in  $\text{Gly}_4\text{H}^+$  cannot be disrupted by bonding  $\text{D}_2\text{O}$  to the oligomer and the complex dissociates on a picosecond time scale at 300 K. Hence, the relay mechanism cannot be invoked for  $\text{Gly}_4\text{H}^+$  and  $\text{D}_2\text{O}$  is unable to promote facile H/D exchange of this (or any larger) oligomer.

#### Effects of Off-Resonance Excitation on H/D Exchange.

The effect of off-resonance excitation on the rate and extent of H/D exchange was studied for several oligomers with  $\text{D}_2\text{O}$  and

(48) PM3 calculations predict a protonated N-terminus  $\text{Gly}_2\text{H}^+$  is 8.1 kcal/mol more favorable than a species with the amide oxygen protonated and solvated.

(49) Molecular dynamics calculations were performed with Hyperchem.<sup>35</sup>

$\text{CD}_3\text{CO}_2\text{D}$ . For  $\text{Gly}_3\text{H}^+$  reacting with  $\text{D}_2\text{O}$  and  $\text{Gly}_4\text{H}^+$  reacting with  $\text{CD}_3\text{CO}_2\text{D}$ , initial activation of the protonated parent appears to decrease the rate of deuterium exchange. This is consistent with exchange mechanisms that proceed via long-lived collision complexes. High translational and vibrational energies of the protonated oligomer reduce the likelihood of forming a hydrogen-bonded collision complex.<sup>23</sup> The failure of collisional activation of  $\text{Gly}_4\text{H}^+$  to promote exchange with  $\text{D}_2\text{O}$  is consistent with this viewpoint. The excess excitation that opens the solvated oligomer by breaking the intramolecular bonds also inhibits hydrogen bond formation to the  $\text{D}_2\text{O}$  exchange agent. Without adduct formation, exchange does not occur. In several instances in Table 1 it is noted that the first exchange is slower than the second. We believe that this results from the ions having excess vibrational and translational energy when they are initially isolated for studied. The complexity of these experiments did not facilitate the addition of a buffer gas to relax the ions prior to studies of the exchange kinetics. Vibrational relaxation is a very slow process. It is promoted most effectively by the exchange process in which a long-lived complex is formed and dissociates.

### Conclusions

We have examined the H/D exchange of protonated glycine oligomers with  $\text{D}_2\text{O}$ ,  $\text{CD}_3\text{OD}$ ,  $\text{CD}_3\text{CO}_2\text{D}$ , and  $\text{ND}_3$  in a Fourier transform ion cyclotron resonance mass spectrometer. Although it is not the sole determining factor, the rate and extent of isotopic hydrogen exchange increases with increasing basicity of the exchange reagent,  $\text{D}_2\text{O} < \text{CD}_3\text{OD} < \text{CD}_3\text{CO}_2\text{D} < \text{ND}_3$ .  $\text{D}_2\text{O}$  is the more discriminant reagent, while  $\text{ND}_3$  exchanges all of the labile hydrogens of all the species studied. For those glycine oligomers whose proton affinities differ from the deuterating reagents by less than 20 kcal/mol, H/D exchange predominantly occurs via formation of a strong hydrogen-bonded species. For those oligomers whose proton affinities differ from the reagents by significantly more than 20 kcal/mol, the exchange mechanisms are more subtle. Our results are in general agreement with the related studies of Lebrilla and co-workers.<sup>22</sup> While these studies were in progress Nibbering and co-workers<sup>50</sup> presented results for  $\text{D}_2\text{O}$ ,  $\text{CH}_3\text{OD}$ , and  $\text{ND}_3$  undergoing H/D exchange with a number of dipeptides and related compounds. Our results are also in reasonable agreement with theirs, and they also discuss an "onium" ion mechanism for H/D exchange.

Five mechanisms are proposed for the H/D exchange of protonated glycine oligomers with reagent bases: the onium ion, relay, salt bridge, flip-flop, and tautomer mechanisms. These processes are summarized in Figure 16. An onium ion mechanism is proposed for protonated glycine oligomers exchanging with basic reagents (such as  $\text{ND}_3$ ), in which a nominally endothermic proton transfer from the N-terminus is accompanied by simultaneous solvation of the resultant onium ion (i.e., ammonium ion). For reagents such as  $\text{D}_2\text{O}$  whose proton affinity is too low to overcome the endothermicity of proton transfer from the peptide, a relay mechanism in which the deuterating reagent shuttles a proton from the N-terminus to a slightly less basic site (amide oxygen) is proposed. Semiempirical calculations indicate that exchange of the amide hydrogens is slightly less favorable than exchange of the N-terminus. A tautomer mechanism is proposed in which a proton is transferred from the N-terminus to an amide carbonyl in concert with transfer of the amide proton to the reagent base. This mechanism is highly favorable for  $\text{ND}_3$ , in which the

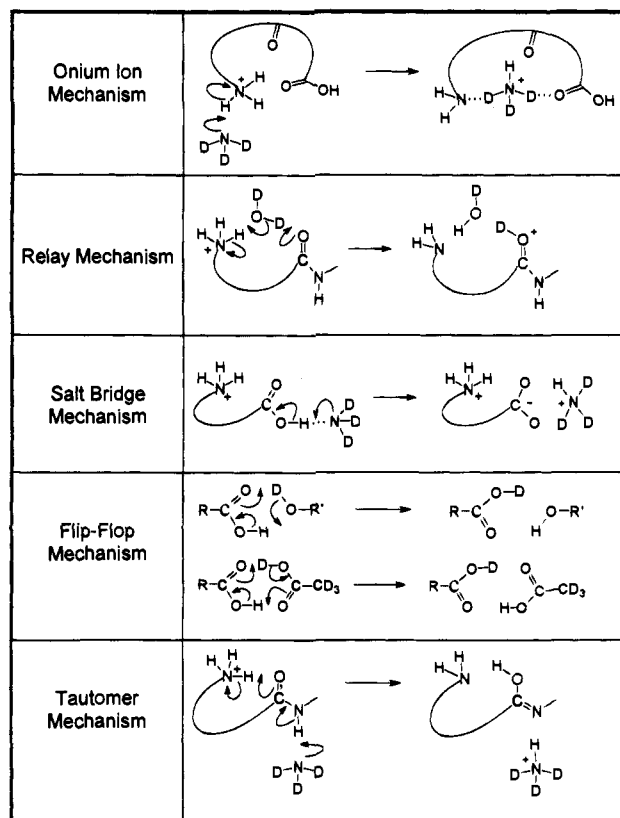


**Figure 16.** Summary of the proposed H/D exchange mechanisms for the glycine oligomers with reagent bases.

ammonium ion is solvated by the tautomerized peptide. Exchange of the C-terminus hydrogen using basic reagents occurs via a salt bridge mechanism, in which the hydroxyl proton is transferred to the exchange gas, creating an ion pair stabilized by a nearby charge center. Exchange of the C-terminus using less basic reagents is slow and probably occurs via a multicentered flip-flop mechanism.

There has been considerable interest in the structural and functional roles of salt bridges in proteins. Charged amino acids have been implicated as factors contributing to protein stability, as driving forces for protein-protein interactions, and as key factors in enzyme mechanisms. The question of salt bridge formation in the gas phase is an interesting one. We believe that H/D exchange intermediates proposed for betaine are perhaps the first examples of salt bridge formation in the gas phase. We also estimate that it is energetically feasible for the C-terminus hydroxyl of betaine and the glycine oligomers to undergo H/D exchange via an intermolecular salt bridge with the deuterating reagent. The systems in which we have invoked salt bridges as viable reaction intermediates involve proton transfer in an acid-base complex to form an ion pair which is stabilized by a nearby charge center.<sup>47</sup> Semiempirical calculations, however, indicate that salt bridges in the isolated glycine oligomers considered in this study are unlikely. This conclusion is supported by the exchange results of oligomers methylated at the C-terminus, which exhibit no difference in reactivity from the unmethylated oligomers. In contrast, the presence of very basic residues such as arginine (whose side chain has a proton affinity 30 kcal/mol greater than the N-terminus) in peptides may allow the formation of intramolecular gas phase salt bridges in peptides with appropriate arrangements of amino acids.

It is particularly interesting to note that  $\text{D}_2\text{O}$  does not undergo facile exchange with the  $\text{Gly}_n\text{H}^+$  oligomers with  $n > 3$ . However, McLafferty and co-workers<sup>17</sup> report that multiply protonated peptides (+6 to +18) of cytochrome *c*, myoglobin,

(50) Gur, E. H.; Dekoning, L. J.; Nibbering, N. M. M. *J. Am. Soc. Mass Spectrom.* 1995, 6, 466.

and ubiquitin undergo extensive deuterium exchange with D<sub>2</sub>O. They observe H/D exchange rates in the range from  $2 \times 10^{-13}$  to  $4 \times 10^{-12}$  cm<sup>3</sup> molecule<sup>-1</sup> s<sup>-1</sup>, with the highest charge states exhibiting the fastest exchange. For peptides with a charge state of +7 or +6, the exchange rates were  $<10^{-12}$  cm<sup>3</sup> molecule<sup>-1</sup> s<sup>-1</sup>, which is slower than the range of rates monitored in our experiments. The Coulomb repulsion between charge sites in a multiply protonated peptide effectively reduces the proton affinity of the species. Williams and co-workers<sup>51</sup> have recently examined the deprotonation energetics of multiply charged cytochrome *c* ions. They observe that the gas-phase basicities range from 234 kcal/mol for the +3 charge state to 192 kcal/mol for the +15 charge state. Hence, exchange of hydrogen for deuterium with D<sub>2</sub>O becomes energetically more favorable. The extent to which protonation sites in these complex molecules are stabilized by intramolecular hydrogen bonding remains uncertain, making it difficult to assess details of H/D exchange mechanisms with different reagent gases.

H/D exchange processes involving even simple model peptides are highly complex processes. As a result, any temptation to assign gas-phase structures of biological molecules from H/D exchange results must be approached with caution. With a thorough understanding of the gas-phase structures and H/D exchange mechanisms of simple glycine oligomers, it is appropriate to proceed with the investigation of larger, more

(51) Schnier, P. D.; Gross, D. S.; Williams, E. R. *J. Am. Chem. Soc.* **1995**, *117*, 6747.

complex protonated peptides. The incorporation of strongly basic amino acid residues, such as arginine and histidine, into the peptides should complicate simple mechanistic pictures of H/D exchange, due to their high proton affinities. The resultant disparity in functional group basicities will mitigate against the relay mechanism for H/D exchange. Exchange via the onium ion mechanism will only be viable when the energy recovered by solvating the onium ion exceeds the combined energy lost from unfolding the peptide and transferring the proton to the reagent gas.<sup>52</sup> We are currently undertaking investigations to elucidate the H/D exchange mechanisms of more complex singly and multiply charged protonated peptides.

**Acknowledgment.** We gratefully acknowledge the financial support of S.C. from a NIH-NRSA traineeship in Biotechnology, of M.T.R. from a California Institute of Technology Consortium grant, and of E.M.M. from a Rainin Fellowship and NIH-NRSA Human Genome traineeship. This work was supported in part by the National Science Foundation under Grant No. CHE-9108318. Funds for instrument development have also been provided by ARPA and DoD-URI programs under Grant No. ONR-N0014-92-J-1901. We are indebted to the Beckman Foundation and Institute for the initial funding and continuing support of the research facilities.

JA943476P

(52) Campbell, S.; Beauchamp, J. L. To be submitted for publication.